THE EFFECTS OF ITO SURFACE MODIFICATION ON LIFETIME IN ORGANIC PHOTOVOLTAIC DEVICES AND A TEST SETUP FOR MEASURING LIFETIME

A Thesis
Presented to
The Academic Faculty

by

Sinan Mahmut Sutcu

In Partial Fulfillment
of the Requirements for the Degree
Masters of Science in the
School of Electrical and Computer Engineering

Georgia Institute of Technology
August 2010

THE EFFECTS OF ITO SURFACE MODIFICATION ON LIFETIME IN ORGANIC PHOTOVOLTAIC DEVICES AND A TEST SETUP FOR MEASURING LIFETIME

Approved by:

Prof. Bernard Kippelen, Advisor
School of Electrical and Computer Engineering
Georgia Institute of Technology

Prof. Oliver Brand
School of Electrical and Computer Engineering
Georgia Institute of Technology

Prof. Shyh-Chiang Shen
School of Electrical and Computer Engineering
Georgia Institute of Technology

Date Approved:

To my grandfather, Rifat Serdaroğlu, the most amazing engineer I have ever had the honor of knowing.

ACKNOWLEDGEMENTS

I would like to thank my advisor Prof. Bernard Kippelen for supporting me and giving me the opportunity to conduct research in this lab. The atmosphere in this group was one of the friendliest and best I have encountered and it was truly a pleasure working here. I would also like to thank the committee members, Profs. Shyh-Chiang Shen and Oliver Brand, for their time and effort. I would also like to thank Prof. Brand for starting off my research experience in Georgia Tech as an undergraduate and exposing me to this environment early on. I would like to thank my colleagues in the lab, especially Dr. Dengke Cai for his work on the lifetime measurement setup with me and William Potscavage Jr., for teaching me everything I know about device fabrication and helping me with depositions. I would also like to give a special thanks to my parents for encouraging me over the years and supporting me in all my endeavors.

TABLE OF CONTENTS

LIST OF TABLES

LIST OF FIGURES

LIST OF SYMBOLS AND ABBREVIATIONS

OLED	Organic Light Emitting Diode
AMOLED	Active Matrix Organic Light Emitting Diode
UV	Ultra Violet
IR	Infrared
C_{60}	Buckminsterfullerene
ITO	Indium-Tin-Oxide
CuPc	Copper Phthalocyanine
CdTe	Cadmium Telluride

SUMMARY

Though relatively young, the field of organic electronics is a rapidly growing market and considerable research is being done in creating a whole range of devices from organic molecules from organic field effect transistors to LEDs to photovoltaic devices. The field of organic photovoltaic in particular has become important in recent years with the push for newer, renewable sources of energy to end the dependence on fossil fuels. While the efficiencies of organic photovoltaic devices continue to rise, one barrier to their commercial adoption has been the limited lifetimes of these devices. While certain degradation methods of organic photovoltaics, such as photo-oxidation, have been extensively studied and solutions to these problems, such as encapsulation, are being researched, certain other degradation mechanisms are less understood and studied. The focus of this thesis is on one such degradation mechanism, UV degradation, specific to the ITO-pentacene interface in pentacene/C_{60} organic photovoltaic devices. Attempts were made to increase the lifetime of the devices by using phosphonic acids or oxygen plasma to modify the surface of the ITO. While conducting these experiments, the lack of a system to test the lifetime of multiple devices for long periods of time became apparent. As such as system was a requirement for future research into the lifetimes of organic photovoltaic devices a system was designed and built. The system would operate the photovoltaic device in a way comparable to its end-use and would allow over 100 devices to be tested simultaneously for durations exceeding 10,000 hours if necessary. This system would allow for statistically significant lifetime testing to be carried out in the future.

CHAPTER 1

INTRODUCTION

The first section of this chapter will serve to familiarize the reader with organic semiconducting materials and will broadly discuss the properties of the materials and the physical mechanisms behind how they carry charge. The second section will introduce the reader to solar cells and important parameters within this field. It will then discuss organic solar cells in particular, their importance to the field and problems specific to these devices. The purpose of this chapter is to give the reader a background into the actual research done for this thesis.

Organic Materials

History of Organic Semiconductors

The first synthetic polymer created in a lab was Bakelite, created by Leo Baekeland in 1907 [1]. Since then many other synthetic polymers have been created and are actively used in people's everyday lives. It was always assumed that polymers would be non-conducting materials. The discovery that opened up the field of organic electronics, however, negated this assumption. In 2000, the Nobel Prize in Chemistry went to Heeger, MacDiarmid and Shirakawa for their groundbreaking 1977 publication on the electrical conductivity of polyacetylene, which they found could be increased by several orders of magnitude through doping [2]. This led to the discovery of a variety of new molecules and polymers that were either intrinsically conducting or with semiconductor properties. These materials have allowed the modern field of organic electronics to grow into an almost billion dollar per year industry where conducting

organic molecules are now used in a variety of different applications from organic light emitting diodes to field effect transistors to solar cells.

Advantages and Disadvantages

One of the key strengths of organic materials is the ability to fine-tune their material properties by changing their molecular properties. By changing the chemical structure of the molecule various properties of the material can be added, removed or adjusted. For example, the addition of side groups to a molecule can make it more soluble thus allowing it to be processed in solution. Similarly other side groups can affect properties like the melting point, brittleness, freezing point, elasticity, absorption or emission spectra and conductivity of the final molecule or polymer chain. By attaching dissimilar moieties, functional groups, on opposite ends of the conjugated system such as NH_2, OCH_3, and OH that donate electrons, and NO, NO_2, CHO, and CN that accept electrons, the molecule can be made asymmetric. This asymmetry allows the molecule to exhibit second-order nonlinearities that results in highly colored compounds that, for the most part, absorb and emit light in the visible spectrum; these molecules are also known as chromophores [3]. Therefore, unlike inorganic materials whose spectra are dependent on their band gap, the absorption and emission spectra of organic materials can be fine tuned by adjusting the side groups of these molecules.

The processes for adjusting the associated side chains of a molecule are well known and documented. Because there are a very large number of molecules and side chains permutations there is a correspondingly large variety of materials properties available [4]. This allows for optimization of an organic material's band gap and thus their optical properties. Comparatively, the range of wavelengths that emission and

absorption occurs on is larger in inorganic crystals, such as silicon. On the other hand, this range is very difficult to adjust in inorganic crystals as it is dependent on the material's band gap and thus changes often require either doping or alloying the crystal and can negatively affect its electrical properties [5]. The same is not true for an organic molecule whose spectrum can easily be altered through changes in the moieties and while most only operate in the visible spectrum, with the exception of some that operate in the near-IR spectrum, it is important to remember that almost half the irradiance of the sun, 497W/m^2, falls in this range [6].

The huge number of moieties available and the permutations of their location on the organic molecule can also act as a disadvantage when compared to inorganic materials with fixed properties; much work must be placed in creating new materials and characterizing their properties. Significant time and expense must be put into determining the most useful side groups and where they are positioned on a molecule.

Another disadvantage of most conductive organic molecules is that they will react in the presence of oxygen or water molecules when subjected to energy, i.e. heat or light, although the rate of reaction varies significantly [7]. This means that any device utilizing organic materials must provide a means of isolating them from the presence of ambient air. This can be done in a number of ways: operating the devices in a vacuum, in a nitrogen or other inert gas environment, or by encapsulating the device to prevent contact with outside atmosphere.

Charge Transport in Organic Semiconductors

To understand the charge transport mechanism in an organic, conducting film one must first consider how the molecule itself is held together. In an organic molecule, the

bonds between the atoms are covalent and are formed by a pair of shared electrons. A carbon atom has four valence electrons: one in the 2s-orbital and three in the 2p-orbitals. This means that a carbon atom will form four bonds in order to fill its electron shell and conserve a neutral charge on the atom. When these covalent bonds are formed with four separate atoms the 2s- and 2p-orbitals can form four sp^3 hybridized orbitals at a lower, preferred energy level. These hybridized states will contain all four electrons in equally shaped orbitals with each electron covalently bonded to a separate atom by a σ-bond. In some cases carbon can form two or three bonds with the same atom; these are known as double and triple bonds. In the case of a double bond, the 2s- and two of the 2p-orbitals mix to form three sp^2 hybridized orbitals that form σ-bonds; the remaining 2p-orbital will form the second bond of the double bond and this bond is referred to as a π-bond. In the case of the triple bond, the 2s- and one 2p-orbital mix to form sp^1 hybridized orbital and the remaining two 2p-orbitals act as the second and third π-bonds on the triple bond. Figure 1 shows σ- and π-bonding in double and triple bonded molecules. It is important to note that π-bonds are significantly weaker then σ-bonds, which can be explained from a quantum mechanical perspective by the degree of overlap of the orbitals. In σ-orbitals the p- or s-orbitals in the atoms forming the bond overlap causing a strong interaction, whereas π-orbitals are semi-delocalized, meaning their orbitals do not overlap to the same extent, and are weaker [1].

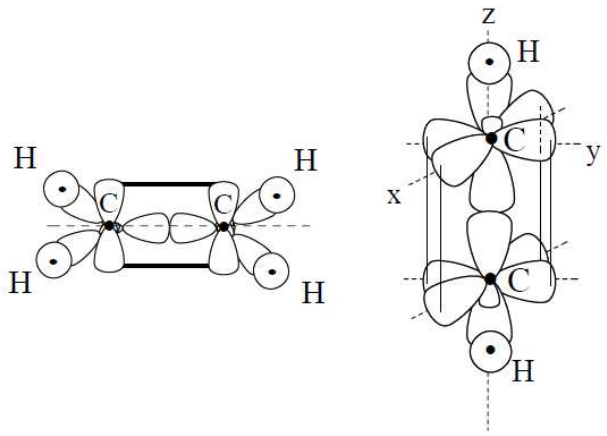

Figure 1: A diagram of an ethylene molecule (left) and acetylene molecule (right) with π-bonds represented by solid lines and σ-bonds by overlapping electron clouds adapted from [1].

For an organic film to be conductive the molecules in the film must consist of a conjugated backbone; this consists of a continuous line of alternating single and double bonded carbon atoms, as seen in Figure 2. This means that each carbon atom has three σ-bonds and one π-bond making them sp^2 hybridized. Due to the weakness of the π-bond, the π-electrons are effectively delocalized, allowing for charge to flow through the molecule. This is due to the fact that the overlap of the unhybridized p-orbitals in the double bond will create a lower energy bonding orbital for the π-electrons as can be seen in Figure 3 known as molecular π-bonding and anti-bonding orbitals.

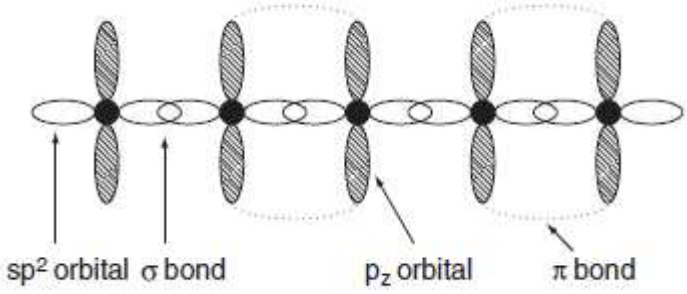

Figure 2: Diagram of a conjugated molecule with alternating single and double bonds, from [8].

This backbone of molecular π-bonding states form a band like structure of overlapping π-electrons. Most of these organic materials form amorphous or semi-crystalline films that lack the repeating crystalline structure found in inorganic crystals. Because of this, the π-bonding states do not form a true band structure with allowed and forbidden states found in inorganic crystals; however, the idea of a π-band structure can be a useful approximation. The level actually occupied by the π-electrons is analogous to the valence band and is known as the Highest Occupied Molecular Orbital (HOMO) level. The anti-bonding π^* band is equivalent to the conduction band, which is called the Lowest Unoccupied Molecular Orbital (LUMO) [9].

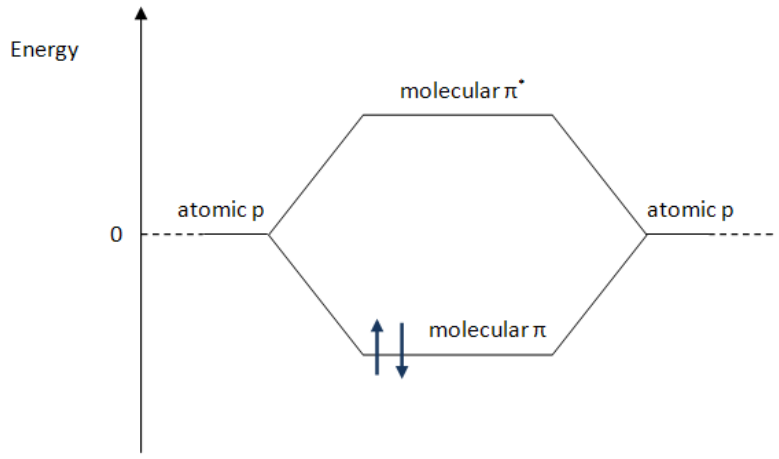

Figure 3: Bond energy diagram and creation of lower energy π-bonding orbital.

The band gap would be the energy difference between the two, similar to an inorganic semiconductor. Thus electrical conduction takes place along the band of π-orbitals within

each molecule, which can then lead to charge transfer between two separate molecules, extending the bands across the entire film.

The actual mechanism for this charge transfer is known as the disorder formalism and takes place through localized hopping of charges between excited and ground state molecules. The charge is represented as a radical ion, which is associated to a local geometry relaxation because of large energetic and positional disorder. The charge then hops from molecule to molecule at a given rate, with each hop totally independent of its previous ones. This is the key mechanism that governs electron transport in these materials; because the charge transfer takes place through a series of completely random hops, mobility values in organic semiconductors are far lower than in inorganic crystals [10,11].

Potential Device Applications

Despite these low mobility values, organic molecules are still being used in the design of organic field effect transistors because of the need for flexible electronic devices that cannot be achieved with crystalline materials due to their brittleness and high processing temperatures. Similarly organic LED displays have become a common place in the last several years and can be found as the backlight in many cell phones, including the newest generation of smartphones such as the HTC Desire and Google's Nexus One that both have AMOLED displays [12]. This has come about because of a combination of space requirements and improved contrast over LCDs previously in use [13]. Finally, organic photovoltaic devices have also been in development as the push for clean, renewable energy has driven more research into the photovoltaic field in general. Organic efficiencies have been slowly catching up to their inorganic counterparts, with recent

efficiencies as high as 7.9% being reported [14]. Less work has been done, however, on another key aspect, device lifetime, which will be just as important in determining whether or not the technology will be adopted. It is these devices and this area in particular that this thesis will further explore.

Photovoltaic Devices

Market Need

Global energy consumption is on the rise and is projected to double from 17TW in 2009 to 30TW in 2025, with the majority of the energy being consumed in countries such as India and China [15]. In addition, the majority of the energy being generated on the planet (~92%) comes from non-renewable energy sources such as coal, oil and natural gas, with only 7% being obtained from renewable sources such as wind and solar. Despite the fact that the sun deposits over 120,000TW/yr, more than enough to meet the world's energy needs, solar energy only accounts for less than 1% of the world's power grid. It would only require a solar farm with an efficiency of 10% covering 1.6% of the area of the United States to meet the countries total domestic energy needs [16]. The growing energy demand, coupled with increasing photovoltaic device efficiencies, has driven market demand in the last several years for solar cells. Between 2007 and 2008, US sales of photovoltaic systems doubled, from $1.7 billion to $3.4 billion and this number is expected to keep rising [17]. It is therefore imperative that research continues so that device efficiencies and lifetimes can be increased and materials and production costs can be decreased in order to ensure that photovoltaic systems can become competitive in the energy marketplace.

Fabrication

One of the biggest advantages of organic materials from a fabrication standpoint is the ability to work with them in thin-films. They can be fabricated orders of magnitude thinner than crystalline silicon, which accounted for 67% of photovoltaic sales in 2008, in the range of hundreds of nanometers vs. hundreds of microns [18,19,20]. This means that substantially less material is needed in device fabrication, allowing for potentially lower materials costs with a commensurate decrease in the overall price per kilowatt hour. The price can be further decreased in fabrication because many organic molecules are soluble in solution and thus can be batch processed in large quantities in solution, such as through inkjet printing. In addition, both their ability to be made thin and their low processing temperatures means that organic electronics can be made on flexible substrates, such as plastics [4].

Conventional solar cells can be fabricated from a variety of different materials, each with their own advantages and disadvantages. Currently, most solar cells are made from silicon for a variety of reasons: it has high charge mobility, longer lifetime, and is air stable. Silicon also dominates the semiconductor electronics market so the infrastructure and fabrication knowledge base already exists. The tradeoff for these advantages, however, is higher materials costs and greater degree of difficulty in processing and fabricating the cells, although batch fabrication is possible. Crystalline silicon is an indirect band gap material, making its absorption less efficient, and also cannot be produced in thin films; while amorphous silicon can its absorption spectrum is also defined by its fixed band gap. These processing limitations and the inefficiency

associated with its indirect gap have driven the search for alternative materials. One key class of materials in this search is organic, semiconducting molecules and polymers [5].

The ability to utilize low fabrication temperatures in the production of organic photovoltaic devices offers the advantage of processing at lower costs and with reduced complexity, especially with regards to batch processing. It also allows processing to be done on a variety of substrates, such as plastics, not open to most inorganic materials. Fabrication of these devices falls under two main categories: thermal vapor deposition and solution processing. Thermal vacuum deposition involves heating up the organic molecules in a crucible inside of a vacuum chamber until they begin to evaporate, whereupon they rise up and are coated on predetermined surface areas of a substrate using masks. The same chamber can also be used to deposit the metal cathode. Thermal vacuum deposition can be used to deposit organic materials one by one into thin-films of several layers or can co-deposit multiple materials simultaneously to form a blend. The films tend to be more uniform and precise thicknesses can be achieved because of tightly controlled deposition rates. Batch fabrication by this method is more difficult, however, because the number of samples processed at one time is limited by vacuum chamber size and deposition rates are relatively slow, usually below 10 Å/s. Processing from solution overcomes these batch-processing limitations because it allows deposition through either spin coating or inkjet printing. These and similar techniques already used in many other commercial applications for "roll to roll" processing will make organic electronic batch processing from solution inexpensive. One downside to solutions, however, is a larger degree of irregularities across the film due to non-uniform blending of the constituent

molecules and variations in thickness due to changes in film density and substrate wetting caused by difficult to control depositions [10].

Important Parameters in Photovoltaic Devices

When discussing any photovoltaic device, regardless of the materials it is made of, there are a number of key parameters that must be understood: short-circuit current, open-circuit voltage, fill-factor, efficiency and output current. All of these parameters can be extracted from a plot of the current-voltage characteristics of the device under illumination such as the one seen in Figure 4. From the data gathered to make this plot it is possible to extract an equivalent circuit model, shown in Figure 6, which includes a diode and current source to model the solar cell and incoming photons, and series and shunt resistors to model parasitic losses [21].

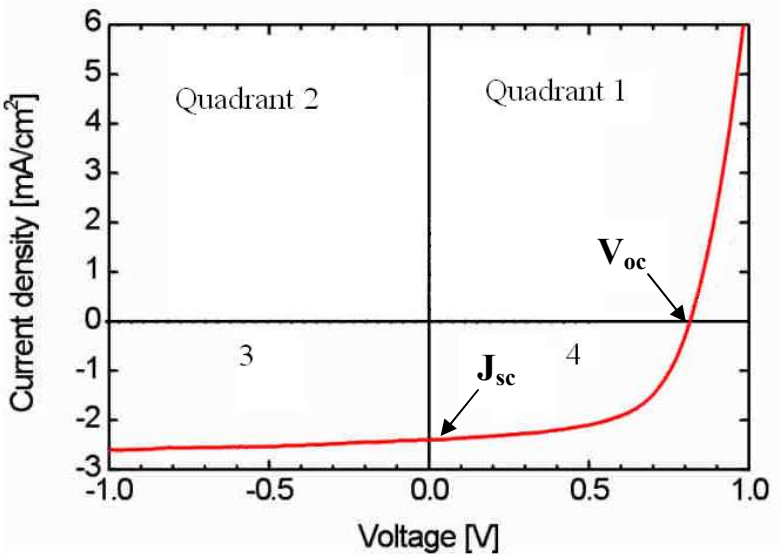

Figure 4: A plot of the current-voltage characteristics of a pentacene/C_{60} photovoltaic device under illumination with important parameters labeled.

One of the most important parameters to consider from the plot is the short circuit current: the current running through the device under illumination with zero bias. At zero

bias, the entire device current is caused by the incident light being absorbed. Therefore, provided the series resistance is not too high, the short circuit current will be equivalent to the light, or photon, induced current I_{ph}. This current is represented in the device model by a current source I_{ph} (as shown in Figure 5).

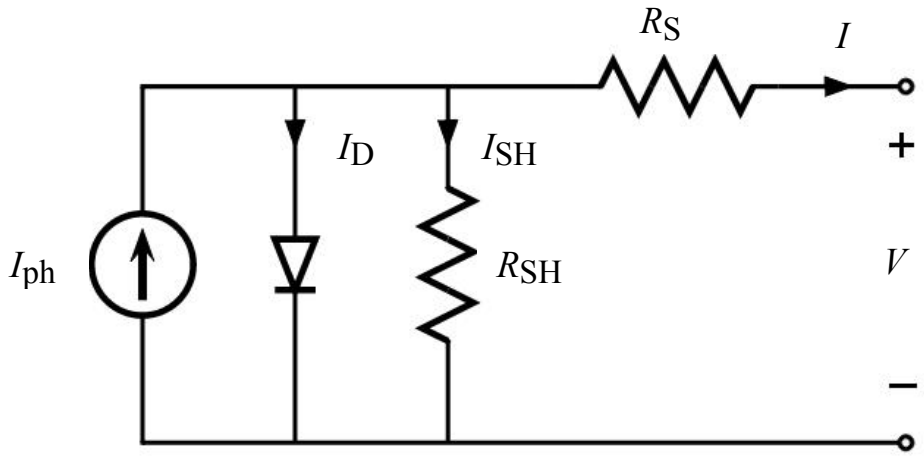

Figure 5. Equivalent circuit model of a photovoltaic device under illumination.

It is important to understand how the photocurrent affects the overall current of the device; in first approximation, the total current passing through a solar cell under illumination can be written as Eq. 1. The reverse saturation current, I_0, is intrinsic to each device, as is the diode's ideality factor, n. The values of the elementary charge, e, and Boltzmann constant, k, are constant, while the temperature, T, and voltage across the solar cell, V, can be varied. It is also important to note that the total current is equivalent to the current through a diode minus the current being created by incident photons.

$$I = I_0\left(e^{\frac{eV}{nkT}} - 1\right) - I_{ph} \tag{1}$$

It is again clear from the equation that when the voltage is zero the total current is equal to the photocurrent. Another variable that is directly affected by the photocurrent is the open circuit voltage. This voltage directly impacts the efficiency (a larger value is preferred). The open circuit voltage is determined as the voltage where the total current through R_S is zero. Equivalently it is defined as the voltage when the current through the forward biased diode is equivalent to the photocurrent. By setting $I = 0$, Eq. 1 can be rewritten into Eq. 2, which is a first approximation for the open circuit voltage.

$$V_{oc} = \frac{nkT}{e} \ln\left(\frac{I_{ph}}{I_0}\right) \tag{2}$$

With the exception of I_{ph} and T all of the other variables in the equation are either physical or device constants and therefore cannot be changed. It can be seen from the equation that open-circuit voltage is dependent on I_{ph} and the diode characteristics. Therefore, any degradation in the value of the photocurrent and diode will also cause the open-circuit voltage to degrade.

This plays an important role in the efficiency, η, of the device, which can be calculated using Eq. 3, where P_{solar} is the incident power onto the cell. It is clear from the equation that higher values of the short-circuit current and open-circuit voltage are desired.

$$\eta = \frac{FF(I_{sc}V_{oc})}{P_{solar}} \tag{3}$$

It is also important to maximize the value of the fill factor. The fill factor is intrinsic to each device and is a measure of how close is the maximum power point, described below, is to the short-circuit current and open-circuit voltage; the value of the fill factor will always be less than 1, this being an ideal device, but the higher the value the higher the

efficiency of the device. This value is affected by the parasitic effects within the device and can be optimized by reducing the series and increasing the shunt resistances [21]. The value of the fill factor is given by Eq. 4, where, P_m, is the maximum power point of the device.

$$FF = \frac{P_m}{J_{sc}V_{oc}} \tag{4}$$

To find this point, one must consider again the current-voltage plot in Figure 4; solar cells can be operated in one of three quadrants as shown on the plot: either the 1st, 3rd or 4th. It is also important to note that power is the product of current and voltage and that for a device to output power that product must have a negative value. Therefore, the only way for a solar cell to actually output power is if it is being operated in the fourth quadrant. When taking the current-voltage characteristics in the fourth quadrant into account, there is an optimal current and voltage value on the curve which will produce the greatest power, P_m.

Photocurrent Generation in Organic Photovoltaic Devices

The most common form of an organic photovoltaic cells consists of two organic light-absorbing layers in between a transparent, conducting anode, usually made of a conducting oxide such as indium-tin oxide (ITO), and a low work function metal cathode. The organic layer closest to the ITO typically exhibits electron donor properties and provides efficient hole transport, while the layer closer to the cathode exhibits electron accepting properties and efficient electron transport. The two organic layers can either be planar heterojunctions or can be blended together to form a bulk heterojunction [22]. As

mentioned above, the overlapping π-orbitals create HOMO and LUMO levels, analogous to the valence and conduction bands respectively, which coupled with the electrodes, form a structure, similar to inorganic p-n junctions, seen in Figure 6.

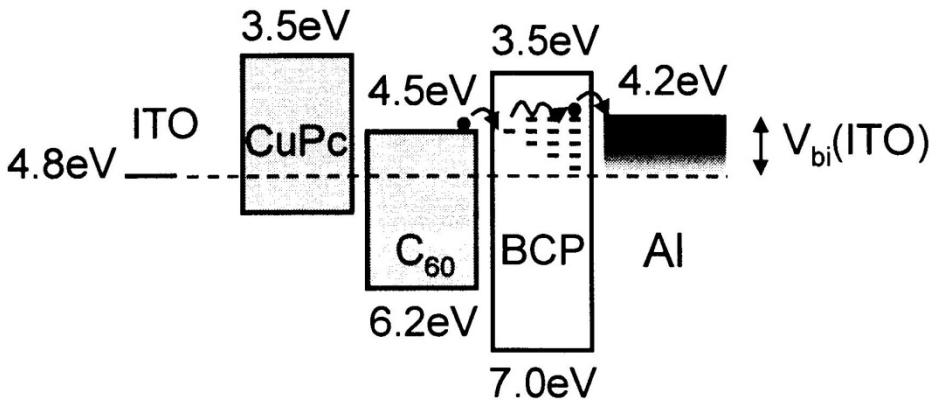

Figure 6: A CuPc/C_{60} planar heterojunction device with a BCP exciton blocking layer to improve carrier collection at the cathode, adapted from [23].

A photon can be absorbed in either organic layer, though each layer will favor absorption in a certain spectrum. The absorbed photon will promote a molecule into an excited state, whereupon the molecule will thermalize into the lowest excited energy state. Once in the lowest excited state, which can either be a triplet or singlet state depending on the molecular structure and morphology, an exciton is formed. The exciton is an electron-hole pair that is coupled with a binding energy, on the order of a few tenths of an eV, thereby maintaining a neutral state. For comparason the thermal energy, kT, at room temperature (T=300K) is 0.026eV. In most inorganic semiconductors, the exciton binding energy is lower than kT, thus the exciton is immediately dissociated and creates free electrons and holes. This is not true in organic materials because of the low dielectric

constants of the materials, the significant electron correlations in both the ground and excited states, and the geometry relaxation associated with the exciton's formation [10].

This lack of immediate dissociation decreases the mobility of the charges, thereby resulting in less free charge carrier production from exciton recombination losses. This is because the exciton is electrically neutral and it is prevented from traveling via drift in the electric field of the device. Thus they must instead diffuse through the organic layer by either Dexter or Förster random hopping interactions, depending on whether they are singlet or triplet excitons, until they reach the interface between the two organic materials. Dexter energy transfer takes place over short ranges and is an exchange interaction between triplet excitons at adjacent sites. This means that the exitons in the two molecules will actually switch, causing the previously excited molecule to be in the ground state and the previously ground state molecule to be in the excited state. Förster interactions are the result of long range electrostatic coupling of excitons between excited and ground state molecules and are the primary energy transfer method for singlets. In this case, both molecules retain their original excitons; however, the excited exciton's energy is transferred to the ground state exciton, causing the two molecules to switch states [11].

Due to the lower charge mobility values of organic materials and the fact that diffusion to the interface is taking place through random hops there is a risk that the exciton will recombine resulting in no photocurrent. It is important, therefore, to ensure the organic layer thickness, and thus the distance the exciton must travel to the interface, is lower than the exciton diffusion length. In materials with low diffusion lengths bulk heterojunctions can be used to decrease recombination losses; the blending of the two

materials ensures that the distances between the organic layers interface is shorter than a planar structure. This also maximizes the surface area of the interface and hence the probability that the exciton will diffuse to the interface before recombining.

Upon reaching the interface an exciton will dissociate to the energetically favorable side. For example, an electron in the donor material will cross into the acceptor material because its LUMO level will be at a lower energy level. Exciton dissociation is in reality a complicated process. There are a wide variety of factors that can influence whether or not this dissociation is energetically favorable, and therefore the rate at which dissociation takes place [24]. If dissociation does occur, the exciton binding energy is overcome and the exciton becomes an electron and hole that will travel via drift and diffusion to their respective electrodes. They will travel in the form of a radical ion that will hop from molecule to molecule, as described by disorder formalism, until they are collected at their respective electrode [25].

Breakdown Mechanisms

The average lifetime for silicon based solar cell is 25-30 years [26]. Unlike an organic semiconductor crystalline silicon as a material is assumed to be nearly 100% stable. The only time this assumption is not valid is for extraterrestrial operation, where issues from cosmic radiation can play a role. The main breakdown mechanisms, therefore, are almost all mechanical: mechanical stress caused by thermal fluctuations, mechanical damage from storms, hail or other materials being thrown at or on the panel and breakage of interconnects due to bending. The only real materials issues are: (i) metal electrode migration through constant flow of current through the electrode over the course of several decades and (ii) chemical breakdown mechanisms via corrosion of the

electrodes or interconnects. Thus all the breakdown mechanisms associated with inorganic materials stem from the packaging of the photovoltaic system and are not intrinsic to the materials themselves [27].

The same cannot be said of organic semiconductor systems, which in addition to the problems associated with packaging also have their own specific material degradation issues. One of the greatest barriers to the adoption of organic photovoltaic systems is the inherent instability of these devices when exposed to ambient air, an environment that contains oxygen and water. As stated earlier, conducting molecules have alternating single and double bonds, which makes them susceptible to reactions with oxygen and water in the atmosphere. Some of the key breakdown mechanisms are associated with this exposure including damage to the metal cathode and photo-degradation of the organic layers, which occurs when a molecule of oxygen or water comes into contact with the organic molecule and a photon. The photon acts as an energy source to overcome the energy barrier of the reaction by optically exciting the organic molecule, which then leaves it susceptible to giving up its π-electron to either oxygen or water, forcing it to form a new σ-bond with that molecule [1]. These interactions are a serious concern for a number of reasons, the most important of which is that these reactions interrupt the conjugation of the molecule's backbone. Conductive organic molecules rely on conjugation as the means of electron transport and any interruption will lead to decreased mobility and an inability to conduct charge, thus severely degrading device performance. The level of degradation is dependent on where on the molecule the reaction occurs as well as the number of sites involved. Another key issue is the change in material properties; the addition of side groups to the molecule will change its

properties with potentially serious consequences to the performance of the device. These changes can adversely affect the materials absorption or emission spectrum or the mobility of the device [10]. Which molecule the organic semiconductor will prefer to interact with, the rate of the interaction and the physical site of interaction are all dependant on and specific to the organic molecule in question, as well as other environmental factors such as concentrations of oxygen and water in the air and the intensity and wavelengths of the photons involved. This complexity makes modeling these interactions a futile exercise without limiting parameter space by physically conducting experiments to determine the rate limiting reaction mechanisms involved.

Lifetime

When determining the commercial viability of a solar cell technology, arguably the most important metric is the end cost per kilowatt hour. To make widespread adoption of photovoltaic systems a reality, the cost must be near or on par with the current cost of electricity supplied from conventional means. One of the largest costs when investing in inorganic photovoltaic system is the initial cost of the system and its corresponding installation; the remainder of the cost of the system is maintenance, this latter being a relatively small fraction of the system's overall cost [27]. This means that in order to reduce the cost of the energy supplied, the system must have as long a lifetime as possible to prevent system replacement or exceptionally high maintenance costs. This is less of a problem in inorganic solar cells whose breakdown mechanisms are limited to the device package. Organic materials also have the same packaging issues while also having their own unique breakdown mechanisms that must be considered. In order for organic materials to compete with inorganic materials for photovoltaic devices it is imperative

that these additional breakdown mechanisms be controlled. Therefore either the device lifetimes associated with these mechanisms must be on par with the package lifetimes or the materials costs must be low enough to justify shorter lifetimes associated with organic breakdown mechanisms. The research conducted in this thesis focuses on the former in an attempt to increase the lifetime of the organic device by reducing the effects of the organic breakdown mechanisms.

CHAPTER 2

CASE STUDY OF A PENTACENE DIODE

Introduction and Current State of Research into Pentacene Based Devices

A significant amount of work has been done to create high efficiency organic photovoltaic devices using fullerene (C_{60}) as an acceptor layer coupled with copper-phthalocyanine (CuPc) in particular. These materials would be layered in planar heterojunction layers in the form of ITO/CuPc/C_{60}/BCP/Al where the BCP is an exciton blocking layer to prevent injection from the aluminum back into the organic materials. Efficiencies of 5% have been achieved in this arrangement [19]. As discussed earlier, one key issue when considering the viability of an organic material for use in an organic photovoltaic device is its exciton diffusion length. Unfortunately, CuPc and other phthalocyanine based materials have low exciton diffusion lengths of <10nm and therefore function best when used in bulk heterojunction devices [28,29]. The tradeoff to this improvement in efficiency is the decrease in stability in bulk heterojunctions, which degrade almost twice as fast in ambient air, as well as when exposed to ultraviolet light, as planar devices [30]. Thus the need for a donor material with a larger exciton diffusion length led to the adoption of polycrystalline pentacene films, whose exciton diffusion length can be as large as ~60nm allowing them to be used in a planar device configuration (ITO/Pentacene/C_{60}/BCP/Al). In addition, this material has a higher film absorbance than materials in the phthalocyanine group. The polycrystalline nature of the

film also allows for the potential for high mobilities, with field-effect mobility values of 1.5 cm^2/Vs demonstrated in highly ordered films [31].

Thus pentacene would be a more efficient candidate to replace CuPc in planar heterojunction devices; however, in this configuration CuPc devices still tend to be more stable in ambient air than pentacene [30]. Pentacene device efficiencies degrade three times faster than CuPc devices in ambient air when in a planar heterojunction configuration [7]. Therefore, in order to create devices to utilize the increased exciton diffusion lengths and the crystalline nature of pentacene, it is important that the issues in device stability of pentacene-C_{60} photocells be addressed.

This research has important implications for the field of organic photovoltaic devices through both the improvement of planar heterojunction devices and also a better understanding of degradation mechanisms in organic photovoltaic devices [32]. This was the motivation for my research presented in this section that focuses on reducing the effects of device degradation through the use of surface modifications. The emphasis was specifically on degradation caused by UV radiation at the ITO-pentacene interface and potential ways of mitigating this effect.

Photo-oxidation of Pentacene

Mechanisms

While the degradation method studied in this thesis was not photo-oxidation, it is still important to understand this method as it pertains to all organic materials. It has been well documented over the last several decades that when reacted with oxygen or water

pentacene forms byproducts in the form of transannular endoperoxide and also dimeric peroxide as shown in Figure 7 [22,33].

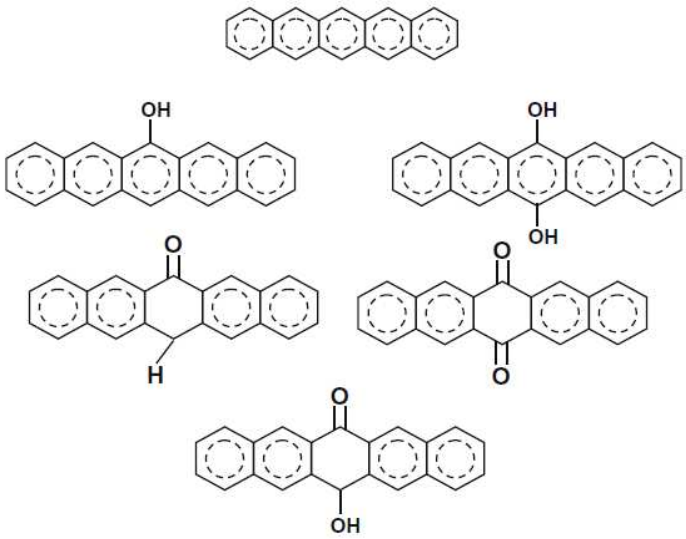

Figure 7: Pentacene (top) pictured with its most common oxidation products, adapted from [34].

There have been debates about what mechanisms actually cause these reactions, but most research agrees that there are two main mechanisms: reactions with oxygen or water in the singlet or triplet excited state of the organic molecule [35, 36]. From a simplified perspective, both reactions involve optical excitation of the pentacene molecule and the elevation of an electron to the triplet or singlet state. This electron then transfers to the oxygen, or water, molecule causing a radical ion to form on both molecules. This charge differential results in the formation of a covalent bond between the two atoms [37,38]. It is interesting to note that in pentacene this reaction almost always occurs in the central benzene ring because of its morphology and polarization is the most susceptible to this interaction [39,40]. When pentacene is in high concentration in solution and is optically excited, for example during fabrication, it is also possible for the molecule to dimerize:

two pentacene molecules will join together by their central benzene rings. This is caused by excitation of the delocalized π-orbitals, but thus far research suggests that this only occurs when pentacene is in solution [41].

Effects on Device Performance and Solutions

The photo-oxidation leads to disruption of the conducing properties of pentacene by two main processes: disruption of the conjugated backbone and addition of new side groups. The first process is the most important because without the conjugated backbone the molecule acts more like an insulator than a conductor, which severely limits the photocurrent. This can be further affected by the addition of new side groups change the absorption spectrum of pentacene, leading to lower total photon absorption rates and a corresponding decrease in current. Finally, these new side groups change the band structure of the LUMO level and create trap states that reduce the mobility.

Currently, there are two main ways of preventing the photo-oxidation of pentacene: the addition of side groups to reduce the reactivity to ambient air or encapsulation of the device to prevent contact with ambient air. The first method is shown in Figure 8 and uses the side group as a blocking molecule, preventing oxygen and water molecules from approaching the reactive site [40]. This method can be problematic because the addition of these side groups usually also negatively impacts the properties of the material, sufficiently altering its device properties to make it unusable in organic photovoltaic cells [42].

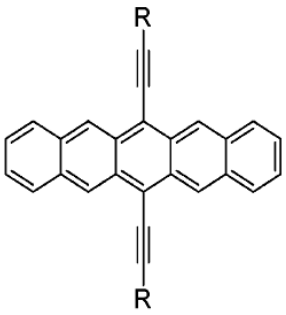

Figure 8: An example of an air stable pentacene oligomer.

Instead of trying to attack the stability problem at the molecular level described above, a macroscopic approach is to fully encapsulate the organic device in a protective layer that allows light to pass through, but prevents water vapor and oxygen transmission. This approach decouples molecular engineering so that improvement in the properties of the molecule's transport need not be sacrificed to increase stability. Finding suitable encapsulation materials that are resistive to both oxygen and water is the most difficult aspect of this line of research although some progress has been made with polymer and metal oxide, such as Al_2O_3, materials [43,44]. Hybrid encapsulation methods using some combination of polymers and metal-oxides have shown effective tolerance in high humidity environments [45].

In conclusion, while photo-oxidations processes are important, much research has already been done in this field. The mechanisms are fairly well understood and clear progress has been made towards solutions to these problems, especially through encapsulation. The same is not true for the next degradation method to be discussed and it is because a lack of progress towards solutions to this problem that my thesis focuses on this topic.

Ultraviolet Electrode Degradation

Mechanisms and Effects on Device Performance

Another key degradation method found in pentacene/C_{60} cells is due to the effects of long term exposure to UV light. The most commonly used transparent electrode in the field of organic optics is ITO and it is almost always grown on a glass substrate. Glass has significant absorption ($\alpha > 0.15$) below 400nm, which means that it will heat up when exposed to UV light [22]. In experiments done by Heringdorf using photoelectron emission microscopy (PEEM) to study the growth of pentacene layers, he noticed that when he left the microscope on for extended periods of time, the UV radiation caused by the photoelectron emission contained sufficient energy to desorb pentacene layers from the ITO coated glass in the span of only a few minutes [46]. It is thought that this effect is caused by the glass substrates, which can absorb significant UV radiation, creating a localized annealing effect caused by the increase in temperature at the interface. This effect can cause pentacene layers closest to the ITO electrode to become thermally unstable, causing reorganization into a different, thermodynamically stable polymorph than in the rest of the film.

Pentacene has at least four different polymorphs, which are characterized by their d(001) spacing. The type of polymorph created by this excessive heating of the interface is one associated with a decrease in spacing when compared to the rest of the film [47]. This decrease in spacing can cause the pentacene to be drawn away from the contact electrode, shown in Figure 9, causing localized reduction in the quality of the contact between the pentacene and ITO molecules. It is important to note that this is a thermal effect, not a UV specific effect, and that in this case the UV light acts only as an energy

source to heat the glass substrate that the ITO is situated on. This means that this UV effect would not be present on substrates that do not absorb wavelengths of <400nm.

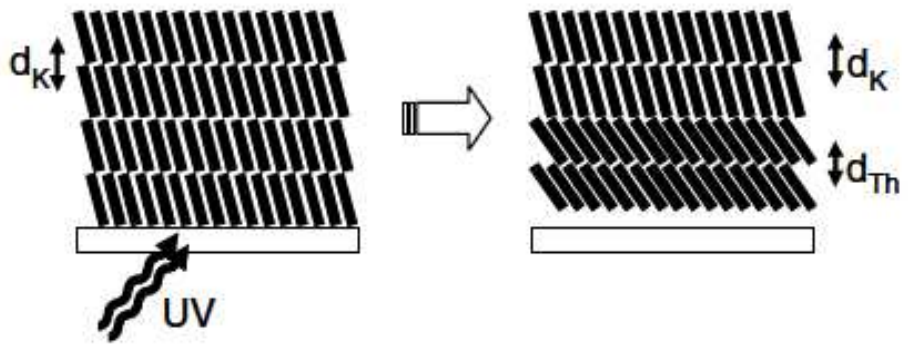

Figure 9: UV degradation of the ITO-pentacene interface resulting in a change in the pentacene crystal and loss of contact with the ITO electrode, from [7].

It is also important to note that this effect is caused by UV radiation and not a result of infrared (IR) radiation. Although IR radiation could be a problem in certain substrates because of the high thermal energy, it is not an issue on ITO coated glass substrates because of their high transmission rates in the IR spectrum, as shown in Figure 10. This means that very little energy in the IR regime is not being transmitted through the substrate, <5%. In addition, the effects of the UV degradation were non-existent when AM1.5G spectrum was used in conjunction with a 450nm high-pass filter. This implies that the higher wavelengths of light in the IR spectrum are not sufficiently absorbed by the substrate to cause the thermal degradation at the ITO-pentacene interface seen with UV radiation.

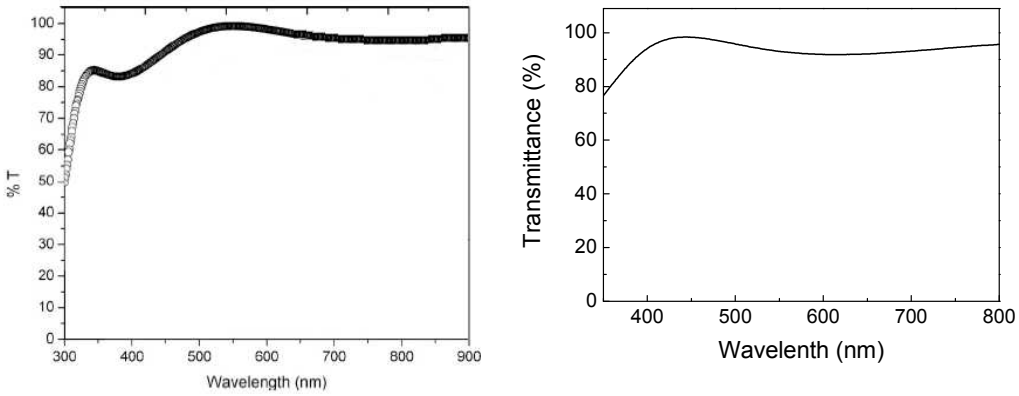

Figure 10: On left, the percentage transmittance of ITO coated glass adapted from [33] and confirmed via measurement, on right, by Dr. Hyeunseok Cheun of the Kippelen Research Group at Georgia Tech.

It is important to note, however, that while the ITO coated glass may not absorb in the IR spectrum, it is certainly possible that the final device package might do so. Therefore if the package is not properly cooled it is possible that the ITO-pentacene interface could be sufficiently heated to cause thermal degradation by IR radiation. This implies that any solutions should focus on minimizing the effects of thermal degradation as there appear to be multiple mechanisms that can cause this degradation.

In fact, this thermal degradation effect is very similar to one also seen in Cadmium Telluride (CdTe) solar cells. In that case, the interfacial damage is between the CdTe layer and the Au back contact and is created when the junction voltage at the barrier saturates as a result of positive bias. This effect results in a corresponding saturation in the device current that can again cause localized increases in temperature and the separation of the CdTe layer from the electrode [48]. In both these cases a contact barrier is formed, which results in an increase in series resistance and a corresponding kink in the current-voltage characteristics that is associated with a decrease in the fill

factor. The fill factor drop over time leads to a corresponding drop in the open-circuit voltage as well as a decrease in the efficiency.

It is possible that another mechanism for thermal degradation in ITO-pentacene interfaces could be as a result of high current densities leading to current saturation through the electrode. It has been shown that charge saturation does occur at the ITO-pentacene interface in these increased current density situations and that these saturation effects can be decreased through changes in the morphology of the ITO. These changes result in increases to the photocurrent through improvements in carrier collection at this interface [49]. Saturation effects typically occur in illuminations of 10-suns or larger [50]. It is possible under these conditions, however, if the morphology of the ITO is left unchanged that localized thermal effects could be created at the interface, leading to similar changes in the pentacene polymorph as those caused by UV heating of glass substrates.

In experiments conducted by Sullivan and Jones on these UV heating effects, the fill factor was found to degrade by 50% within an hour of exposure to UV light of wavelength larger than 370nm, the V_{oc} by 30% and the efficiency by 70% despite the pentacene/C_{60} cells being under vacuum, with no exposure to either oxygen or water. They also found that when they conducted a similar experiment under vacuum with a λ=455nm high pass filter the change in V_{oc}, J_{sc} and FF were less than 3% in one hour and the change in efficiency less than 10% under continuous operation [7]. Thus the thermal damage done to the interface can have a clear, negative impact on the operation and lifetime of these photovoltaic devices.

Potential Solutions

The effects of UV radiation on the ITO contact electrode are a very important factor to device performance and stability. As the study of these effects has been limited to glass substrates, it is unclear whether or not other substrates will have similar effects, though it is highly likely if they have similar absorption characteristics in the UV spectrum. One clear solution to the problem at hand would be to somehow remove the UV component of sunlight and prevent it from coming in contact with the ITO. One option that exists could be to utilize encapsulation materials that absorb UV radiation. Unfortunately such options are problematic because they increase material costs by requiring an additional coating to surface layers. They also increase the difficulty of other packaging degradation issues by increasing the thermal load (through UV absorption) on the solar cell package, which as stated above is one of the key failure points in inorganic semiconductors. Therefore, a preferable solution would be one that addressed the decoupling issues between the pentacene and ITO itself, either by decreasing the effects by ensuring a better contact, or by completely stopping the effect by preventing the energy transfer and annealing effects in the pentacene. The initial goal of this thesis research was to focus on this latter approach of improving the interface to avoid or reduce decoupling of pentacene from the ITO.

Purpose of the Experiment

While the effects of oxygen and water on pentacene degradation have been extensively studied and solutions focusing on encapsulation are being pursued, very little research has been done into decreasing the effects of UV thermal degradation of the ITO-pentacene interface. The goal of the research being conducted has been to see if surface

modification of the ITO could ensure a better contact with the pentacene layer, thus decreasing the effects of thermal damage to the interface. Research has been done on the use of surface modifiers such as oxygen plasma and phosphonic acids on the work function and morphology of ITO and has yielded increased efficiencies and lifetimes in OLEDs devices [51]. In pentacene/C_{60} photovoltaic devices, however, similar modifications have had almost no effect on efficiencies despite increasing the work function of the ITO. Previous studies found that while the actual work function of the ITO was modified within a range of 4.5-5.4eV, the energy barrier height between the modified ITO and pentacene remained constant at 0.6eV. It was hypothesized that this was a result of Fermi level pinning effects and resulted in no change in the open-circuit voltage [52]. No further studies on the long term stability of the ITO-pentacene interface after surface modifications were made. Thus, the goal of our research was to pick up where these previous studies left off and begin to study the effects of surface modifications on the ITO-pentacene interface degradation in pentacene/C_{60} solar cells. The surface modification techniques utilized were the same as those in the papers sited above: oxygen plasma and phosphonic acids.

Before studying the process on something as complicated as a full organic solar cell, it was determined that the best course of action would be to study the effects on only the ITO-pentacene interface, without the additional C_{60} layer. The goal was to create pentacene diodes and examine if the surface modifications would have any effect on the diode lifetimes [53]. The energy level diagram for the pentacene diode is shown in Figure 11.

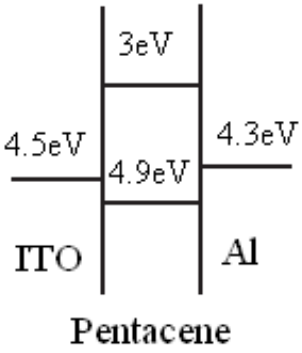

Figure 11: Energy level diagram for Pentacene before surface modification.

Based on the experiments conducted on charge saturation at the ITO-pentacene interface and similar effects seen on CdTe solar cells, it was assumed that under extreme biasing conditions the ITO-pentacene interface in the diode would create localized thermal annealing effects in the pentacene along the interface. This would cause the device to degrade in a similar manner to that of the UV exposed photovoltaic devices. It was also assumed that the rate of this degradation could be affected by changing the ITO-pentacene interface via surface modifications that could improve the contact at this interface by changes in morphology. If there was no difference in degradation rates between different surface modifiers, the experiment would not be continued on to actual photovoltaic devices. If there were differences, the experiment would be conducted using full photovoltaic devices under illumination that would include a UV component for two reasons: (i) to confirm that similar results were being obtained between UV based thermal degradation and current saturation based degradation to prove similar processes are at work and (ii) to prove that surface modifications on the ITO would indeed improve the ITO-pentacene interface.

Device Structure

The device structure can be seen in Figure 12, which consists of a glass substrate coated in ITO, whose surface was either modified or left untouched as a control, followed by a 100nm layer of pentacene and a patterned top aluminum electrode.

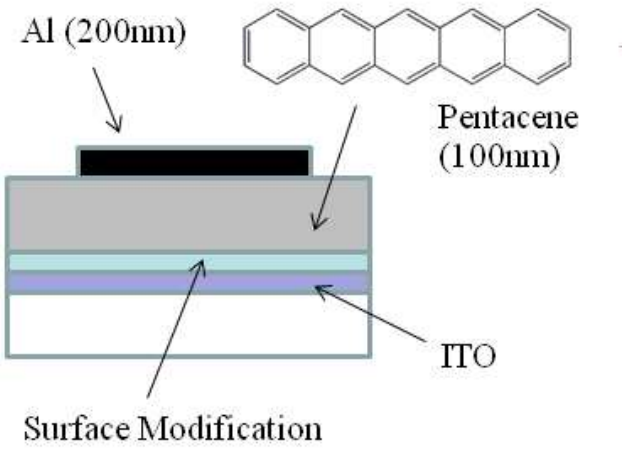

Figure 12: Device structure of pentacene diodes.

The pentacene thickness was selected to be large enough to ensure that the device would exhibit diode like properties. If the pentacene layer was too thin, there could be a risk of a short forming between the metal electrodes creating a device with resistor like properties as opposed to diode like properties. By ensuring sufficient film thickness this risk was mitigated. The device itself consisted of one common anode of aluminum on ITO and five separate cathodes of patterned aluminum on pentacene. As the device was composed of an organic semiconducting layer, it was assumed that charge could not flow outside the region between the two electrodes and therefore each cathode constitutes its own separate device [10]. Thus each diode substrate contained 5 individual devices, though

each substrate only had a single surface modification performed across the entire substrate. Figure 13 is a diagram of a completed device.

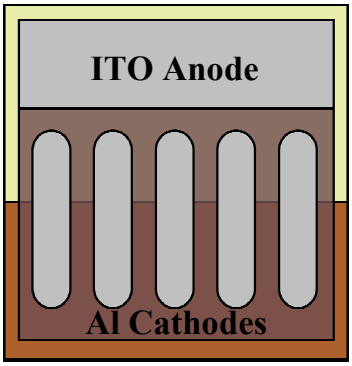

Figure 13: Top down view of a pentacene diode with surface modification.

Sample Preparation

To investigate the effects of surface modification on the long-term stability of the ITO-pentacene interface, the first step was to create samples of diodes with different surface modifications to determine if there was any effect on the interfacial stability. The sample preparation process can be simplified down into four parts: substrate cutting/cleaning, substrate patterning, substrate surface modification and final deposition. When otherwise specified, work was done in an atmospheric glove box in a 99.9% nitrogen environment with <1ppm of both O_2 and H_2O.

Cutting and Cleaning of Substrates

The first step in the process was to obtain a sample of ITO substrate on which to build the actual devices. To achieve this step a 14x14 inch ITO-coated glass substrate

from Colorado Concept Coatings LLC with a sheet resistance of ~15 Ω/sq was cut into 14x1 inch strips, which were then cut down into 0.97x1 inch square pieces; any glass pieces within an inch of the edge of the original square were discarded to prevent non-uniformity. The cutting was achieved by measuring out the correct dimensions on a grid lined table with a glass cutting blade attached.

The samples were then placed in a sample holder and into a pyrex container. The samples were then fully submerged in a series of four different solvents used to clean the samples in the following order: Liquinox in de-ionized water, de-ionized water, acetone and isopropyl-alcohol (2-propanol). Each step was carried out in an ultrasonic bath for 20 minutes and between each step the samples and pyrex container were rinsed off for two minutes with de-ionized water and were blown dry with nitrogen. Liquinox is a laboratory detergent that is phosphate-free and is used to remove organic compounds from the surface of the sample. The acetone and isopropyl-alcohol helped remove any remaining traces of organic substances as well as any remaining Liquinox from the substrates surface. After the final drying step substrates were wrapped using aluminum foil and stored inside the glove box to prevent contamination.

SiOx Buffer Layer Deposition

The next step of the sample preparation process is done to prevent damage to measurement instrumentation rather than device functionality. While measuring the current-voltage characteristic of any organic device, there is always a risk of a punch through of the thin metal electrode and active organic layers. This situation can occur when the probe measuring the cathode applies too much force; it will tunnel through both the top electrode and organic layers and make contact with the ITO anode on the bottom.

This creates a short circuit that can cause damage to sensitive and expensive equipment. To prevent this punch through, the area underneath the top electrode is masked with 300nm of SiOx, as can be seen in Figure 14. With this architecture, even if the probe does punch through the electrode, it will not be able to tunnel through the insulating SiOx film and thus prevents any damage to the equipment.

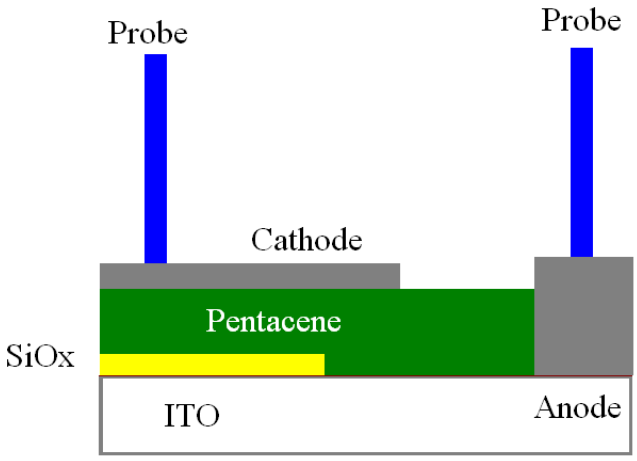

Figure 14: Diagram of protective SiOx layer beneath the cathode probe.

This safety layer of SiOx is grown using electron beam deposition. The samples are placed on a mask that only exposes approximately 40% of the substrate's area. The samples are loaded into the e-beam sample holder and are allowed to reach a vacuum level of $<1.0 \times 10^{-6}$ Torr. Using an AXXIS system by Kurt J. Lesker Company an electron beam is fired at 99.9% pure SiO to deposit a 300nm thick layer on the surface of the ITO-glass substrate at a rate of 5 Å/s.

ITO Surface Modification

Once the substrates were patterned and cleaned, they were ready to be treated with the surface modifiers selected for the experiment. The ITO surface was modified by

one of two different means: mechanical or chemical. The mechanical method consisted of subjecting the ITO layer to an oxygen plasma for 3 minutes in a Plasmatic Systems Inc air plasma chamber. This process raises the ITO's work function by depleting the tin at the surface, thus raising the ratio of indium that serves as a better hole injection material, but also increases the sheet resistance of the ITO, most likely through the loss of the conducting tin [54]. The process also serves to mechanically smooth down the ITO surface, cutting the average surface roughness in half [55]. To chemically modify the surface, a variety of different phosphonic acids were used to modify both the work function and surface morphology of the ITO. The list of phosphonic acids used in these studies is shown in Table 1. All of these acids were produced and obtained from Prof. Seth Marder's research group in the Georgia Tech School of Chemistry and Biochemistry.

Surface Modifier Used	Modified ITO Work Function (eV)
F2BPA	4.4
F5BPA	4.9
F1BPA	4.95
F3PPA	5.15
F3BPA	5.25
CF3BPA	5.3
CF3PPA	5.4

Table 1. A list of phosphonic acid surface modifiers used and their effect on the work function of ITO.

All the phosphonic acids were prepared into solutions and applied to the ITO surface using the same procedure. First, 2 mg of the phosphonic acid in solid form was weighed out on a Sartorius TE124S analytical weight balance and placed in a sterile, sealable beaker, along with a clean stirring magnet. The beaker was transferred into the glove box and 6.6 mL of 99.8% anhydrous chloroform from Sigma Aldrich and 3.4 mL

of >99.5% anhydrous ethanol from Sigma Aldrich was added inside. The beaker's cap was tightly sealed and set on a hot plate/stirrer overnight at 28°C at 350 RPM. The substrates, not more than 4 at a time, were then placed with the ITO side up in a 4" diameter petri dish and the fully dissolved phosphonic acids were poured into the dish onto the substrates. The solution was allowed to evaporate for at least 2 hours at room temperature, or until all the solvent had evaporated off. Annealing of the substrates was then done on a hot plate at 120ºC with the ITO side still up for one hour. After annealing, the substrates were rinsed off in a 2:1 ratio of chloroform:ethanol for 15 minutes and annealed again at 120ºC with the ITO side still up for one hour upon which the surface modification process was complete.

Final Deposition

After surface modification, the substrates were again loaded onto a sample holder with multiple mask layers that were then loaded into the SPECTROS, vacuum thermal deposition system, by Kurt J. Lesker Company. Upon reaching a pressure of $7x10^{-8}$ Torr, the system was used to deposit 100nm of pentacene at 1 Å/s followed by a shadow masked pattern of 200nm of Al to define the cathodes at a rate of 3 Å/s. The actual depositions were made by William Potscavage Jr. of the Prof. Kippelen's research group at Georgia Tech. The completed devices were transferred to a separate glove box for testing by means of vacuum sealed containers to prevent interaction and contamination with the outside air.

Sample Testing and Results

Procedure for Measurement

After being transferred to the glove box for testing, samples were kept in the dark to prevent any photo-oxidation. For measurements the diodes were placed in a sample holder with a common anode and five separate, switchable connections to the device cathode. The selected cathode and anode were directly connected via BNC cables to a Keithley 2400 Source Meter that in turn was connected to a controlling computer via a GPIB cable. The sample holder was again kept in a dark environment, in the glove box, to prevent any photo-generation of carriers under illumination that could affect the results. A National Instruments LabView program was used to control the experiment. The program allowed the user to set a constant current through the device and measure the change in bias voltage at a given time interval. The active area, the area on each device that does not contain SiO_x between the anode and cathode layers, was measured before testing each device and averaged ~0.1cm^2 per device. The average short-circuit current values for the pentacene/C_{60} photovoltaic devices that I created were ~7mA/cm^2 and as previously stated, saturation of the ITO electrode occurs around 10-suns. Therefore, the value of the current through the diodes was set to achieve a current density of 100mA/cm^2, a value that would approximate a solar cell operating at 14-suns. Any thermal degradation caused at the ITO-pentacene interface would create an increase in the contact resistance as the pentacene changed polymorphs and pulled away from the ITO. This change in contact resistance would correspond to an increase in series resistance in the solar cell model. This increase in series resistance would be apparent as

an increase in the bias voltage across the device. Thus degradation of the ITO-pentacene interface could be tracked by this change in voltage.

It was assumed that in the absence of light, oxygen, and water, photo-oxidation of the pentacene could be ignored as the degradation mechanism in these devices [56]. Instead the degradation method was assumed to be caused by charge saturation of the ITO-pentacene interface that would cause thermal damage to the interface. This damage was assumed to be similar to the effects of UV damage as in both cases the damage is caused through thermal processes. The charge saturation would cause a similar, localized thermal affect that would cause a change in the polymorph of the pentacene, as seen in UV degraded devices, leading to the pentacene to pull away from the ITO interface and cause an increase in the contact resistance. Similarly, because the charge injection barrier between ITO and pentacene remained constant for all the different surface modifications applied due to Fermi level pinning, the degree of charge saturation and therefore the associated thermal effects were assumed to be uniform across all devices [53]. Thus any changes in degradation rates could be a result of changes in surface roughness or interface morphology caused by the modifications on the ITO-pentacene interface. The change in voltage over time was recorded and compared based on the surface modifications utilized. Before each experiment was started, the current-voltage characteristics of the diode were measured by a separate LabView program in order to ensure diode like behavior was present and the device was not defective. Each device was tested for at approximately 20 hours of continuous operation at a bias voltage sampling rate of 15 cycles per minute. Each diode contained five devices, though there were instances of defective devices on some diodes.

Results

After completing the experiments, the data was processed to determine the percentage change in voltage between the initial voltage measured across the device and the final voltage after 19 hours. This data was averaged across all devices, 7 devices per modification on two separate substrates, in each category of surface modifications and plotted onto a graph, shown in Figure 15. This graph shows the percentage change from the initial bias voltage to the voltage recorded after 19 hours of continuous operation. This is percent change is plotted vs. the modified ITO work function, with the surface modification used to achieve this work function listed above each point; the error bars represent the standard deviation between the 7 devices. The results that were collected show a difference between the modified work function of the ITO and the rate of degradation of the pentacene diode. The number of devices measured is less than the devices fabricated because of shorts within certain devices; in addition, two of the surface modifiers used to produce devices caused complete failure in the devices: F2BPA and F3BPA. In the case of F2BPA, the work function of the ITO is actually decreased, which caused the devices to behave as a resistor instead of diodes. The devices made with F3BPA had issues with peeling of the top metal electrodes after deposition and further experiments using this phosphonic acid were deemed unnecessary due to the backlog of devices being tested.

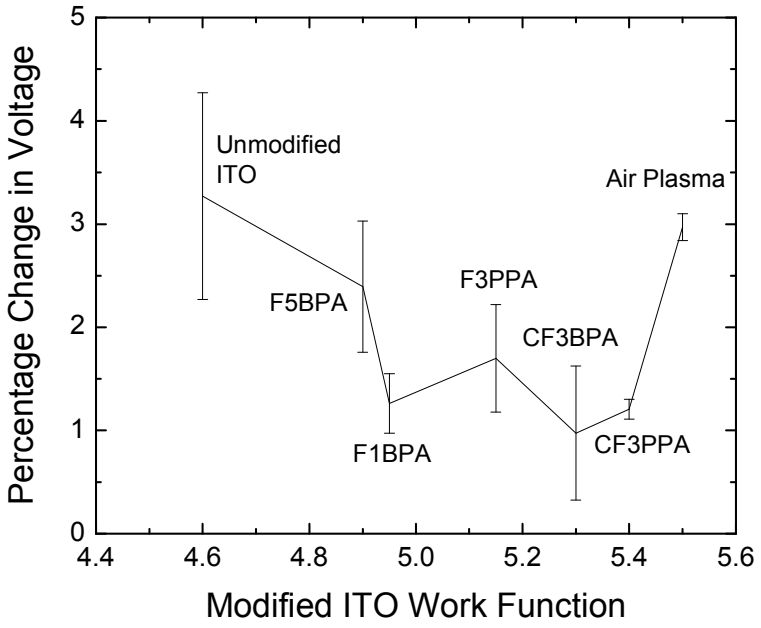

Figure 15: Graph of percentage degradation in voltage verse surface modification used over a 19 hour period.

The graph of the data shows a trend in the work function with regards to lifetime: as the work function of the ITO increases, so does its resistance to degradation. The notable exception to this is the results for air plasma, which seem to perform on a similar level to unmodified ITO. This could be due to a result of an unfavorable change in morphology during surface roughening that occurs with air plasma that does not occur with the use of phosphonic acids. It is also clear that there is a large variation in standard deviation for most of the surface modified devices. This could either be a result of non-uniformities caused by surface modification or could be attributed to small scale variations in processing. Either one could be detected through larger sample sizes; if the standard deviation remains high the issue is probably with the surface modifier. If the standard deviation gets smaller, the issue is probably small variations in processing that would be negated with larger sample sizes. There are several possible explanations for the results

themselves, as to why a trend might exist between surface modifications of the ITO work function and the lifetime of the device.

One possible explanation might have been based on research into modifications to the ITO morphology. This research showed that by improving the ITO-pentacene interface through changes in the morphology of the ITO it was possible to increase charge collection in the device [49]. This was done through small scale roughening of the ITO surface. It is possible that while the injection barrier height remained unchanged, changes in morphology allowed increased charge collection, leading to decreased charge saturation. This decrease in saturation could have slowed the rate of thermal effects, slowing down the degradation of the pentacene at the interface. This would also explain why the oxygen plasma had less of an effect on lifetime because it smoothed out the ITO surface. This can be tested in organic photovoltaic devices by measuring the current-voltage characteristics of the devices under illumination and comparing the short-circuit currents of the devices. This is an unlikely explanation, however, as previous work has shown no change in short-circuit current based on surface modifications. Although this work was limited to fewer phosphonic acids than tested in this experiment, it seems unlikely that there would be a large change in short-circuit current without a change in energy barrier height [52].

Another possible explanation is that while the injection barrier height is held constant when in contact with the ITO due to Fermi level pinning, it is possible that the change in morphology of the pentacene negates these effects. Thus the change in contact resistance from the pentacene pulling away from the ITO might be negated by the increase in charge injection caused by the unpinning of the Fermi level from surface modifications with high ITO work functions. One way to test this theory in the future would be to measure the injection barrier height again after continuous operation to identify any changes that might have occurred.

A final explanation could again lie with the surface morphology of the interface. While the change in morphology might not lead to more charge carriers being collected, it is possible that the change could cause the extent of the lifting off of the pentacene layers to be decreased. If this were the case, better contact between the ITO and pentacene might be maintained, leading to a smaller increase in contact resistance and thus a slower rate of device degradation. This explanation seems the most likely and could be confirmed through a combination of imaging of the interface to determine the extent of the pentacene lift off and more simply through the modeling of the series resistance in the photovoltaic device before and after the lifetime experiment was conducted. If this theory is correct, the increase in series resistance in the device model will be lower in those samples that maintain better contact at this interface. This theory would also explain again why the air plasma had less of an effect on lifetime than phosphonic acids; the decrease in roughness of the ITO could have resulted in an increase in pentacene lifting off when compared to the rougher, phosphonic acid modified ITO.

One aspect of the experiment that could have improved the results, but was not considered until later, was the inclusion of a thermocouple to the ITO-pentacene interface that could monitor changes in the temperatures. While the thermocouple would not be able to sit directly on the junction, it could have potentially been close enough to record any increases in temperature that might have been associated with the excess of charge carriers through the junction causing localized thermal annealing.

In addition, over the course of several months more than 65 individual devices were tested, which corresponded to approximately 1700 hours of continuous testing. While large amounts of data were collected, it was immediately apparent that individual lifetime testing of devices was extremely inefficient. There was a clear tradeoff between the duration of the lifetime testing and the total number of samples that could be tested; this translated to a tradeoff between a statistically large enough sample size to discern a trend among devices and a statistically long enough experimental run time to discern a

clear difference in degradation rates between the devices. This issue was also exacerbated by the attempted scope of the experiment and the large variety of different surface modifiers used: a total of 7 different phosphonic acids, air plasma treatment, and control samples were tested. Therefore while clear results were collected, the experiment would have been better served by decreasing the number of surface modifiers tested and increasing the sample size of each group.

The change in the lifetime with varying surface modifications did, however, make it clear that these modifications do play an effect on lifetime and that they are an interesting area to further explore. Having conducted the experiments, it was also clear that while further research needs to be done it is first imperative that a new means of testing multiple samples at once be developed. The amount of time spent testing individual devices made experimenting on lifetimes far too inefficient because of the sheer amount of time spent gathering data that was not broad enough to have a large statistical significance. Because of the importance of obtaining statistically significant results and the need for a lifetime measurement setup not only for my own experiments, but also for further research within the group, it was decided that future experiments on device lifetime would be placed on hold in favor of creating a lifetime measurement system.

CHAPTER 3

LIFETIME MEASUREMENT SYSTEM

Rationale for a New Lifetime Measurement System

From the previous work completed on the lifetime of pentacene diodes there was a clear lack of equipment necessary for the efficient, long term collection of lifetime data on organic photovoltaic devices. The need for a new lifetime measurement system that would be able to gather data from multiple devices simultaneously was very apparent and before any more experimentation could be done it was obvious that one would need to be designed, built and tested. The first step in this process was determining the current state of the art in lifetime measurements of organic photovoltaic devices. This would then be compared with the requirements of my experiments and the needs of the rest of the Kippelen research group. These requirements would then shape the design of the lifetime test system that would be built and used for characterization of the system.

Current Lifetime Measurement Equipment

In order to begin experimentation into the effects on the lifetime of organic solar cells a new experimental setup needed to be devised that could handle the large amount of samples over the long time durations required to gather statistically significant data. Research into current setups turned up two key pieces of equipment and assumptions used in current lifetime measurement setups: (i) a light source that could mimic AM1.5G spectrum, which is the spectral irradiance of the sun as measured on the Earth's surface,

and the time spent under illumination and (ii) the measuring instrumentation used to determine the current-voltage characteristics and the time period between measurements.

Light Source

A review of literature provided a variety of different light sources that fell into one of three categories: xenon filled gas discharge or arc lamps, high power LED arrays and the actual sun. The key features of all the light sources reviewed were their ability to match the AM 1.5G spectrum as closely as possible, both in terms of wavelength of light as well as the irradiance. Another key requirement was stability so as to ensure that any change in the output characteristics of the photovoltaic device would be due to degradation and not fluctuations in the actual source. The most common setups used in literature were either the use of a gas discharge lamp or the actual sun itself. Both have their own associated drawbacks. In the case of the gas discharge lamp, most of the lamps have lifetimes between 700-2000 hours, with mean degradation before failure between 5-7% of output irradiance. Oftentimes for longer simulations light bulbs would burn out and would be replaced mid-experiment [57]. This meant that when utilizing a lamp, most lifetime tests were done for between 120-300 hours of continuous illumination, with most of those falling on the lower end. In addition, while all these lamps were rated as Class A solar simulators (the non-uniformity of total irradiance must be $\leq \pm 2$ %, the temporal instability of the total irradiance must be $\leq \pm 2$ % and the spectral match in each wavelength internal must be $\leq \pm 25$ %), the standard for the temporal instability of the output irradiance is only valid for 1 hour; the assumption being this is sufficient time to test several devices [58].

In the other case, where the sun was utilized, the draw backs were more numerous. For one thing, it was only truly useful in a location with high solar insolation year round as otherwise the time spent under illumination could decrease up to 40% between the average high and low in the continental United States [59]. This also poses a problem in that solar insolation changes throughout the day and also varies with season, which means that the irradiance on the cell would vary with time, making it more difficult to track the rate of degradation of the device. Another drawback is that the experiment did not involve continuous illumination, as the cell was not under illumination at night and on cloudy days, which could again affect the rate of degradation of the device. Finally, it required that the cell either be housed in a nitrogen environment with access to direct sunlight or it required that the cell be encapsulated. The latter would mean that the researchers could not know if the degradation in the cell was due to interaction with oxygen and water from the breakdown of the encapsulation or because of lifetime issues. It did allow for a greater time span in terms of data collecting; most were conducted between 300 and 750 hours, by far the longest lifetime experiments in literature, but one must take into account again that the device was not under illumination for all these hours [60]. In most cases the encapsulated sample would be placed in a glove box at night, so even the rate of decay due to other factors such as breakdown of the encapsulation would be difficult to ascertain [61].

Measurement Instrumentation

The next important piece of equipment is the instrumentation used to measure and record the actual affect of the source of illumination on the solar cell. In a review of literature, the most common method was to simply measure the current-voltage

characteristic of the device at set intervals. The difference in interval once again depended on the method used for illumination; for example, in cases using sunlight with an encapsulated cell, measurements were often taken only once per day or per week, whereas for those using gas lamps it was more frequent at once every 10 minutes to an hour. None of the systems, however, had any continuous, real time measuring systems in place. In addition, the number of samples that could be measured at one time was also very limited. The largest number of devices that could be simultaneously measured was six; however, this setup consisted of three separate solar simulators, so in actuality each one could only measure two devices at a time [62].

Requirements of a New Lifetime Testing System

When designing the new system the initial goal was to design a setup that would allow the research into UV degradation of pentacene/C_{60} devices to continue. It was clear, however, that a multi-purpose test system capable of running a variety of different experiments simultaneously would be more beneficial to the future of the lab. Thus the system described in the next sections was designed to be used with any organic photovoltaic devices to run continuously monitored tests under illumination, with or without a UV component, over any desired length of time. The system was also designed to operate as many devices as possible at a given time to ensure a statistically large sample size for all experiments being operated.

Measurement Length

The system used to measure the diodes in the studies presented in Chapter 2 was designed to follow a real time voltage change that allowed us to obtain a continuous rate

of decay of the device. The compromise of this approach was that it only allowed the user to measure one device at a time. To conduct an experiment on par with those in published research would require the device to operate under continuous illumination for a period of 200 hours per device. To get a statistically significant number, ~100 devices, would take 20,000 hours, or about 2.3 years. In addition, although the literature search yielded ~200 hours as the standard duration for a lifetime test, one must consider that the average inorganic panel, as previously mentioned, lasts approximately 25-30 years. This translates to roughly 175-200 thousand hours. In other words 200 hours translates into only 0.1% of the lifetime of the device and is not enough time to be able to predict lifetime. This is because the different degradation mechanisms associated with organic materials have different rates; thus, some experiments would require far longer time periods than others. For example, the continuous monitoring method has a specific advantage for studies of UV degradation of the ITO-pentacene interface, because the rate of degradation appears to be a function of time [7]. This time dependent process could be modeled provided a reasonable amount of data could be collected. Thus a longer time span, closer to 2000 hours, which is roughly three months or 1% of the total lifetime of the device, could give sufficient data to create such a model. Photo-oxidation mechanisms, on the other hand, are more difficult to model with time, since they depend on the characteristics of the molecules in the film and its morphology. In addition, factors such as encapsulation must be taken into account, which may require far longer measurement periods. The time requirements could be potentially accelerated by subjecting the devices to harsher conditions, such as higher temperature operation, increased oxygen content or humidity, and removal of encapsulation. Thus the system's

design had to incorporate the ability to operate for much longer time spans, possibly up to or exceeding one year, or 9000 hours depending on the goal of the experiment. To run lifetime tests for such long periods it is imperative that the light source used could be operated for these durations with minimal change in irradiance.

Light Source

Having determined the requirements for the experiments time span, the next step was to select a light source that could operate over the given time span with an appropriate emission spectrum. Because of their limited lifetime, gas discharge and arc lamps were out of the question, since they are usually only designed to operate for time periods no longer than several tens of hours at a time. Another option stated in the literature was the actual sun, but the location of the laboratory in Atlanta, GA made this problematic (in the last 60 years, Atlanta had, on average, 110 cloudless and 107 partly cloudy days distributed fairly evenly among all 12 months, reducing the overall solar insolation [63]). This, coupled with the other disadvantages listed above, makes the sun an unattractive light source in terms of ensuring a continuous, stable source of irradiance. It was determined that the only devices that could meet the lifetime requirements with a stable output irradiance would be surface mounted LEDs. These devices have lifetimes of upwards of 100,000 hours with no more than 30% decay in the intensity of the output light, as can be seen from Figure 16. When operated for less than 10,000 hours this decay is cut in half to 15% change in the light output.

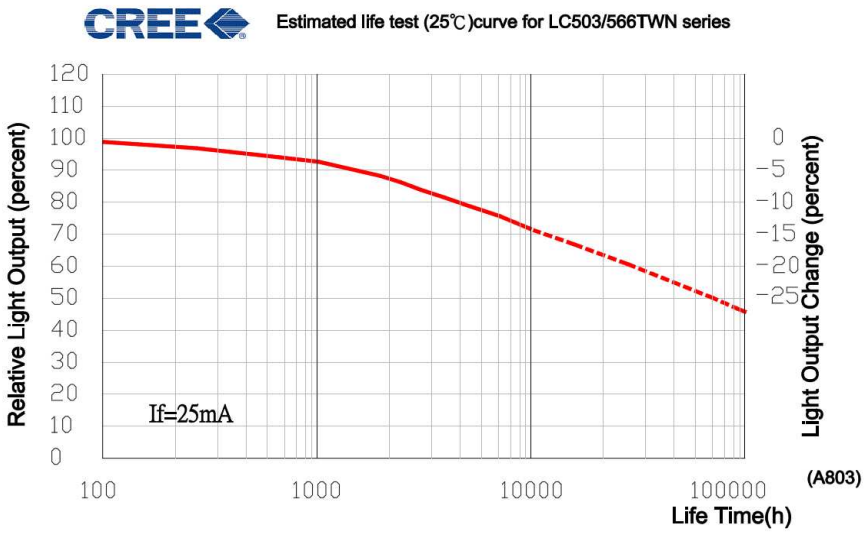

Figure 16: Cree surface mount LED output characteristics with time, taken from [64].

While these devices do not mimic the AM1.5G spectrum, it was clear that this was not necessarily a requirement. The absorption spectrum of most organic photovoltaic devices falls clearly within the visible spectrum, with most molecules absorbing in either the yellow to red range, such as pentacene, or the green to UV range, such as C_{60}. Figure 17 shows a plot of the absorption spectra of both molecules as well as the calculated absorption spectrum of both molecules when combined in a device [18]. As the figure clearly shows, the entire absorption spectrum of the two molecules lies within the visible spectrum, which means that any light outside the visible spectrum is not absorbed.

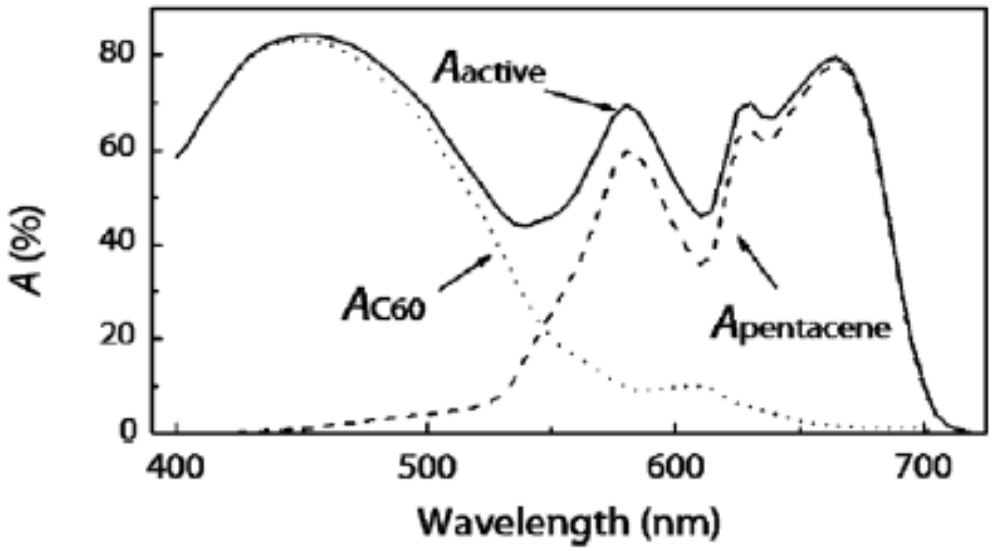

Figure 17: Absorption spectra of pentacene, C_{60} and calculated absorption of the two together from [18].

Therefore, when selecting the surface mount LEDs to use for the lifetime test setup, it was important to find LEDs that output over the entire visible spectrum, which corresponds to a cool white LED. While LEDs in this spectrum work for lifetime tests that do not focus on UV as a degradation mechanism, some experiments like those conducted on the ITO-pentacene interface do require UV illumination. Therefore it is important for the lifetime setup to also include a means of adding an UV source in conjunction or instead of the illumination from the visible spectrum. Thus it was decided that a similar Cree surface mount UV LED would be used to supply UV illumination of the photovoltaic device being tested.

Measured Parameters

After selecting the light source and duration of the experiment, it was also important to determine exactly what kind of information the experimental setup should

record. While most systems in the literature sought to measure the change in current-voltage characteristics when the device was subjected to constant illumination, it was immediately apparent that this setup would not mimic how the device would actually be used in the real world. In situ, solar cells would be connected into series and parallel arrays, in order to supply the correct current and voltage requirements of the load. The devices themselves would be run at or around their maximum power point to ensure efficient operation. Based on this and the desire for real-time, constant measurements of the devices in order to obtain more complete data to track their degradation it was determined that there were two possible setups for measuring the devices: either maintaining a constant bias voltage and measuring the output current degradation or maintaining a constant output current and measuring the bias voltage degradation with time.

The first option has a clear disadvantage: looking back at Eq. 2 we can see that the open-circuit voltage is a function of the photocurrent. This means that any degradation to the photocurrent as a result in the breakdown of pentacene, or some other active layer in another organic material, will result in a decreased open-circuit voltage. While this is not as large an issue for the experiments being conducted on the ITO-pentacene interface, since their open-circuit voltage degrades at a lower rate, the lifetime measurement system being set up must be viable for a broad range of organic photovoltaic experiments. In an experiment where photo-oxidation of active layers and corresponding breakdown in photocurrent does occur, this drop in the open-circuit voltage would cause a drop in the voltage for the optimum power point. This would be further exacerbated by other factors that can affect V_{oc} such as a decrease in the shunt

resistance, R_p, due to the formation of trap states or if an increase in the series resistance causes its values to be comparable to the shunt resistance, which does play a factor in UV damage of the ITO-pentacene contact [65]. If the bias voltage in the experiment were held at a constant value, it is possible that it could exceed the open-circuit voltage. Looking back at Eq. 1 we can see that this would cause the diode current to exceed the photocurrent, which would shift the device operation to the first quadrant; in this case the bias voltage and output current would both have positive values, leading to power consumption rather than production. This would invalidate the basic goal of the test setup, which would be to mimic real world working conditions on the cell.

This is not true for the second operation method, in which the output current is held constant and the bias voltage is allowed to degrade. In this case, while Eq. 2 still holds true and the open-circuit voltage does decay, the bias voltage is allowed to decrease as well, preventing the device from being pushed into the first quadrant. This is also true because the output current is forced to maintain a negative value, holding it in the fourth quadrant until the degradation is so great that the bias voltage drops below zero under illumination, which would imply a certain level of breakdown in the photocurrent. The value for this breakdown can be adjusted as desired through the selection of the output current as demonstrated from Eq. 1; because the output current is held constant, the bias voltage will be equal to zero when the device's photocurrent has degraded to a certain percentage, $P_{deg,\ photocurrent}$, as defined in Eq. 5.

$$P_{deg,photocurrent} = 100\left(\frac{I_{out,selected}}{I_{sc,initial}}\right) \tag{5}$$

It is important to note that the value of the short-circuit current in the equation is measured before the lifetime experiment. The value for the output current would usually be selected as a percentage of the current at the maximum power point to ensure continuity with real world applications, where the stated lifetime of the photovoltaic device would be determined by a percentage of initial power output, usually in the range of 80% [26]. In addition, selecting a value near the maximum power point ensures that time spent running the experiment is minimized, allowing for more samples to be tested in a shorter time span.

System Implemented for Lifetime Testing

Having reviewed the literature to determine the current state of testing equipment and having compiled a list of requirements for the general framework of the test system it then became necessary to actually build a prototype of this test system. The prototype would then undergo testing to ensure that it met all the requirements in the previous section. The next section describes the components of the lifetime setup and their design and function.

Light Source

As stated previously, it was decided that a cool white surface mount LED would have a sufficiently broad spectrum across the visible range to function as the light source for the lifetime test system. In order to ensure that these assumptions were correct and that the LED would not necessarily have to cover the full AM1.5G spectrum, the spectral response of the cool white Cree XLamp LED was measured using an Ocean Optics Spectrum analyzer. The recorded spectrum of the LED was normalized such that the area

under the curve was equal to one. The total output irradiance of the LED was given as 50mW/cm^2 by the manufacturer and this value was multiplied across the recorded spectrum to determine the spectral irradiance. Figure 18 shows a plot of this calculated spectral irradiance of the LED compared to the AM1.5G spectrum across the same wavelength [6]. By integrating the area under the AM1.5G spectrum, we find that the total irradiance for this range is actually 54.3mW/cm^2, a value that is comparable to the white LED.

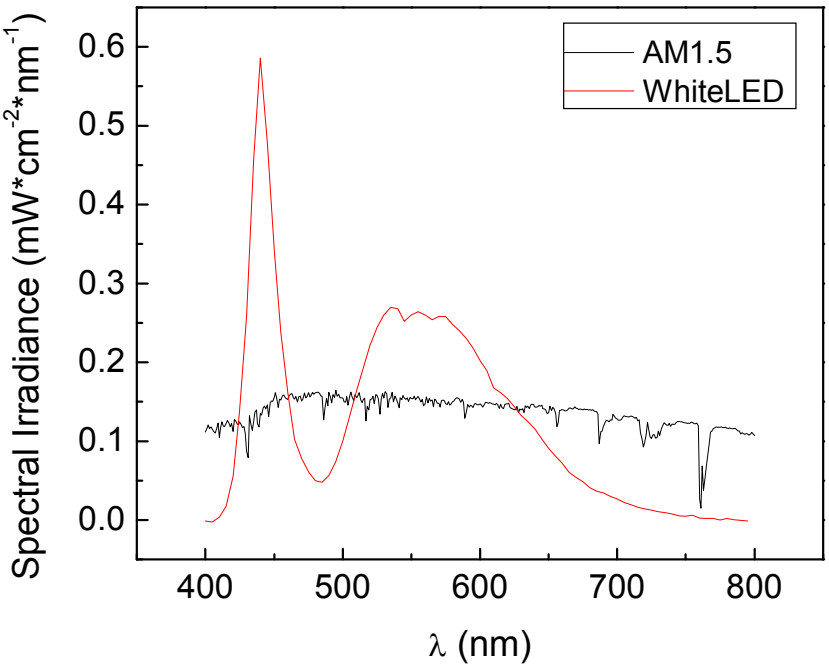

Figure 18: Output spectrum of Cree XLamp surface mount white LED and AM1.5G over the same wavelengths.

As a final test the number of photons emitted by each light source was convoluted with the EQE of the device and integrated over the wavelengths of the light to determine the total number of incident photons/second absorbed by the device over a unit area of 1cm^2.

The number of photons emitted was calculated by dividing the output power at the given wavelength by the energy of a photon at that wavelength to determine the total number of photons at that wavelength. The total number of photons absorbed by the white LED was 8.55×10^{14} compared to 7.86×10^{14} by the AM1.5G spectrum, showing that the white LED mimics AM1.5G spectrum with less than 10% variation in pentacene/C_{60} devices.

In addition to the white LED, a separate UV LEDs can also be incorporated into the test setup to ensure that the effects of UV radiation can either be accounted for or ignored, depending on the experimental setup required. A Cree XLamp LED was again used, only this time the UV series was utilized with an output spectrum shown in Figure 19. Once again the LED output power, 50mW/cm^2, in this range (375-425nm) closely mimics the AM1.5G power at 47mW/cm^2. This allows the user to either focus on the desired degradation method or utilize both LEDs to ensure compatibility with AM1.5G. It is assumed that infrared radiation can be ignored, since very few molecules presently absorb far above 750nm. Nonetheless, the setup does leave room for IR LEDs to be utilized.

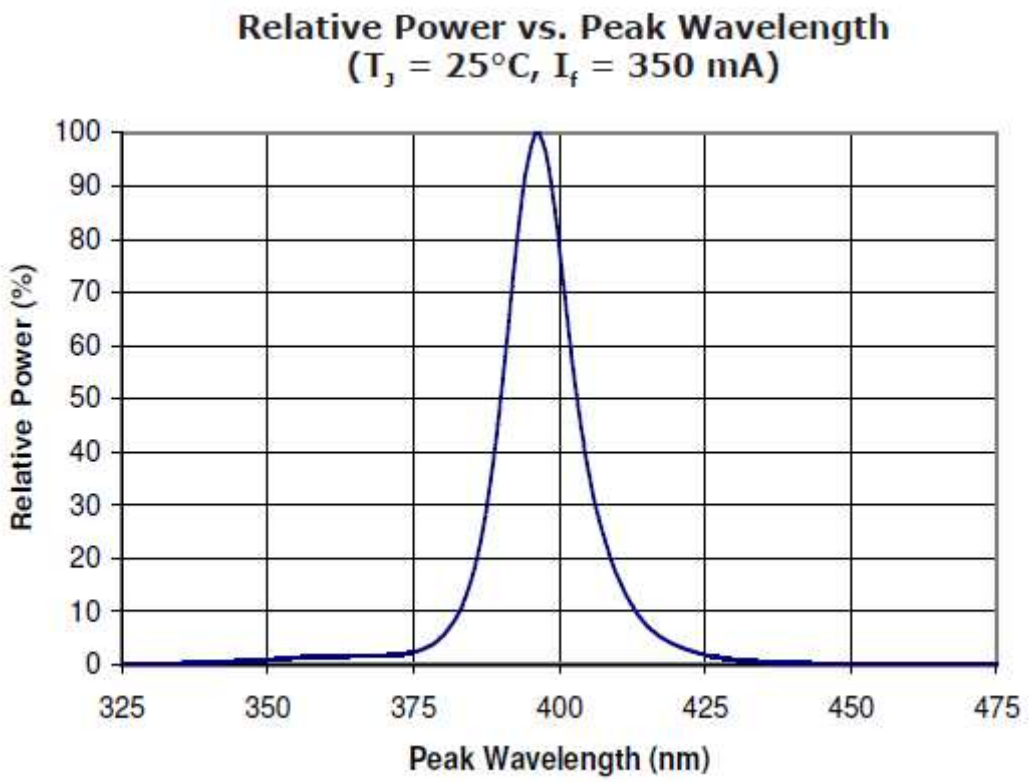

Figure 19: Spectrum of a Cree XLamp UV surface mount LED.

Sample Holder

A suitable sample holder was designed based on others currently utilized in the lab to function as a platform to supply a constant current to the device while measuring the bias voltage across it. The bottom of the sample holder, designed by Dr. Dengke Cai, was fabricated out of aluminum for its low cost and ability to act as a heat sink, and the top was fabricated out of Teflon. The sample holder fully encloses each substrate, which serves the added benefit of shielding the device from any ambient light. It can hold up to 16 substrates at once and each substrate would sit in the sample holder facing upwards with the transparent electrode on the bottom. In order to illuminate the device the sample

holder was designed with a gap underneath each substrate. Sample illumination was achieved by placing the LED underneath the sample holder and allowing light to shine up through this gap, through the transparent electrode and into the device. A schematic of the sample holder can be seen in Figure 20.

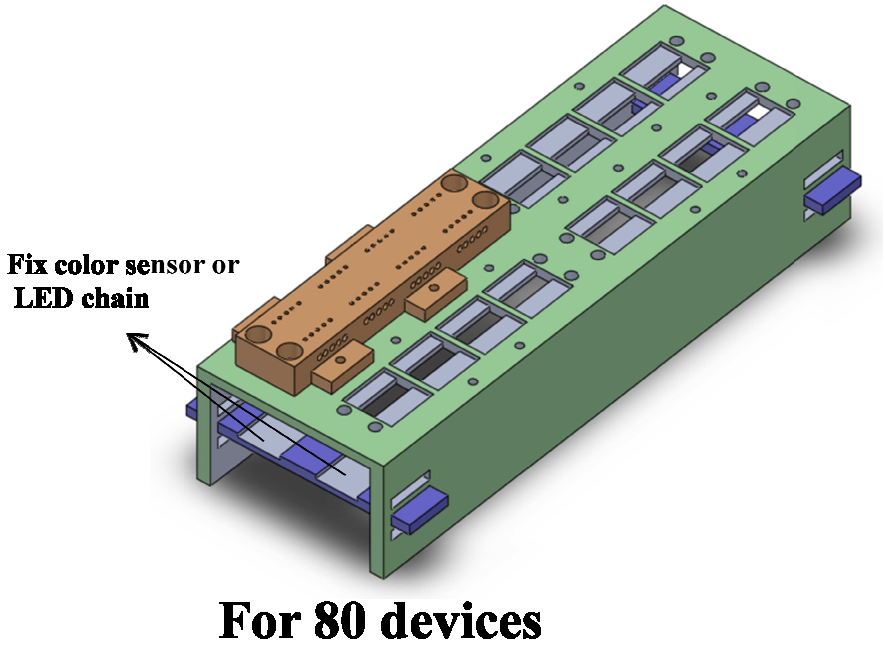

Figure 20: Sample holder designed by Dr. Dengke Cai.

For prototyping purposes a similar sample holder was used, but the prototype could only hold a single substrate and was used to conduct all characterization experiments. In addition, while waiting for the final sample holder to return from the machine shop, temporary sample holders were created out of plastic device holders.

Cooling

To ensure temperature variations do not have an effect in the lifetime system a series of cooling fans and heat sinks were utilized. As stated above, the sample holder

was fabricated out of aluminum as a low cost heat sink and each block of samples was cooled with their own 120mm, 4500 RPM cooling fans, similar to those found in computers. Similarly, the output driver boards and the LEDs were both mounted on hollow, aluminum blocks with their own cooling fans operating underneath as seen in Figure 21. This ensured that the sample holder, LED, and driver boards never exceeded a temperature of 30ºC even after 200 hours of continuous operation with temperatures checked every 24 hours via thermocouple.

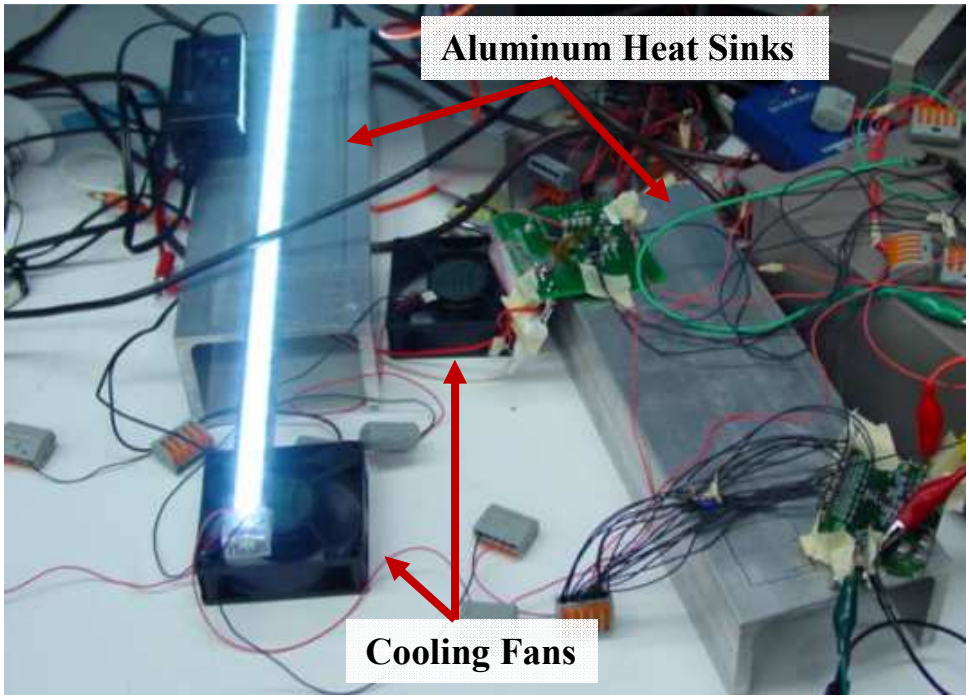

Figure 21: LEDs and driver boards attached to aluminum heat sinks and fans. Under normal operation the fans would be positioned inside the aluminum heat sink.

Output Current Source

The main goal of the test setup was to maintain a constant current through each device on the solar cell's substrate. To achieve this, two different test boards were selected to be used as prototypes. Each printed circuit board had a microcontroller and

the associated circuitry to power it. Both had a set number of outputs that could all be held at the same, constant current, which was adjustable to an extent by an on-board variable resistor.

The first board, an LX1991 Evaluation Board from Microsemi, consisted of six outputs at a constant current ranging from 1.5-30mA at each output and is adjustable by an on board rheostat (R_{set} on the circuit schematic seen in Figure 22). It was immediately apparent that this current was too high, as the maximum power point of the pentacene/C_{60} solar cells translated to a current of 0.4mA or larger. In order to decrease the output current, resistor R_7 was removed and replaced with a 200kΩ rheostat, which would increase the input resistance into the microcontroller. This method allowed the current at each output to drop to as low as 0.3mA and thus could be used for our test purposes. In the process of adding the rheostat, however, the sixth output of the board was accidently shorted out, giving the prototype board only 5 outputs. In addition, it was found after working with the second board that the rheostat was unnecessary and that the current could be limited by sending a pulse signal, with the same amplitude as VDD, through the PWM INPUT port. The manufacturer designed the board so that the duty cycle of this pulse would work to decrease the output current. Tests with a duty cycle of ~2% achieved the desired output currents.

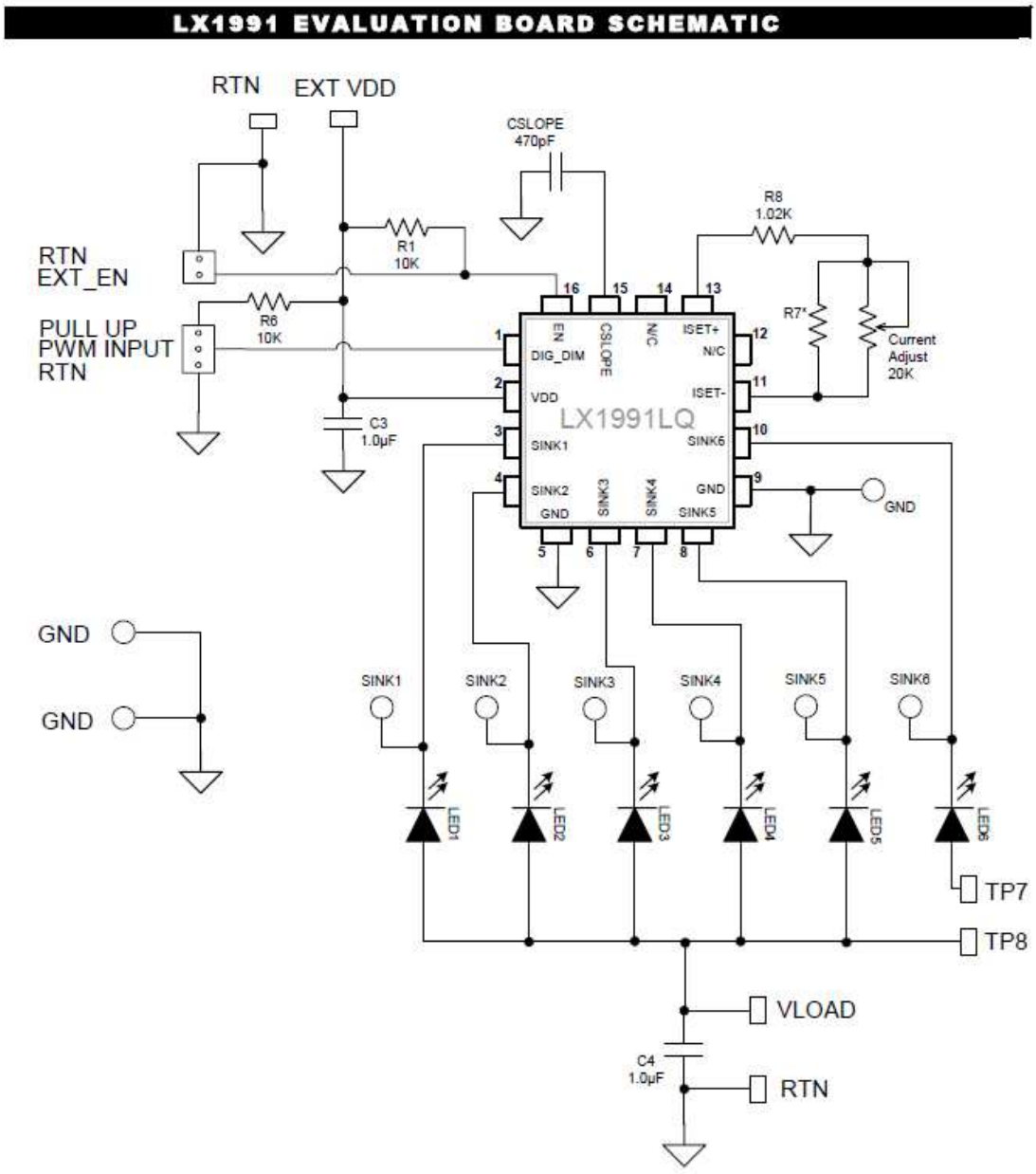

Figure 22: Schematic of Microsemi Evaluation Board taken from manufacturer.

The second board, a MAX16809 Evaluation Board from Maxim Integrated Products, consisted of 16 outputs at constant current ranging from 1-40mA each and was again adjustable by an on board rheostat. Similarly, by applying a pulse signal of voltage of 5V with a duty cycle of ~2% to the PWM input port the current value could be

dropped to 0.25mA at each output, suitably low for the requirements of the photovoltaic devices being tested. A schematic of the evaluation board can be seen in Figure 23.

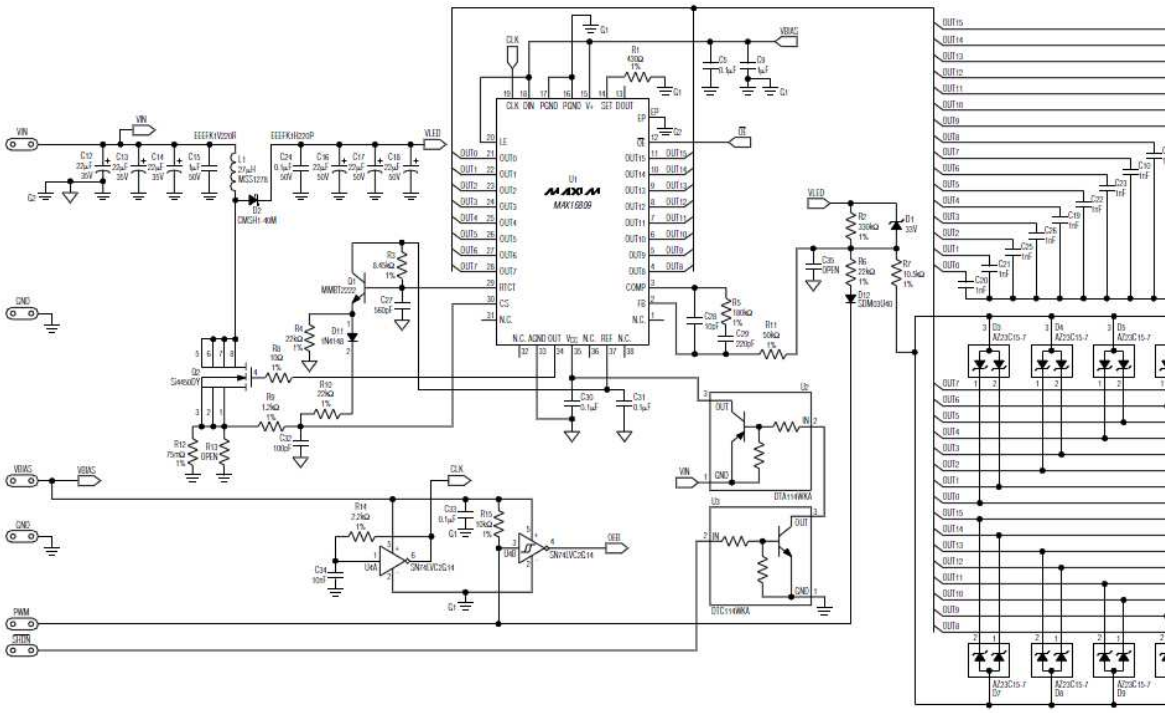

Figure 23: Schematic of Maxim Evaluation Board taken from manufacturer.

Setup

In the experimental setup, the outputs of the current sources were connected in parallel with the Keithley 2700 digital multimeter, which was used to record the output voltage. The positive input of the Keithley was connected to the common ITO anode and the negative input was connected to a single device, with five total on each substrate, cathode. The same was not true for the current sources. Both boards being utilized could only supply positive current; however, to operate in the fourth quadrant and produce power, the device must output a negative current. For the device to produce a negative current, current would need to flow from the cathode, through the active layers and into

the anode. If the current outputs were set up similar to the Keithley, with the positive on the anode and the negative on the cathode, the opposite would be true and current would flow from the anode, through the active layers and into the cathode. To achieve the desired, negative current the polarity of the current outputs had to be reversed. Thus the positives terminals of the current source were connected to the cathodes (one to one for a total of 5) and all 5 negative terminals of the current source were connected to the anode; this is illustrated in Figure 24.

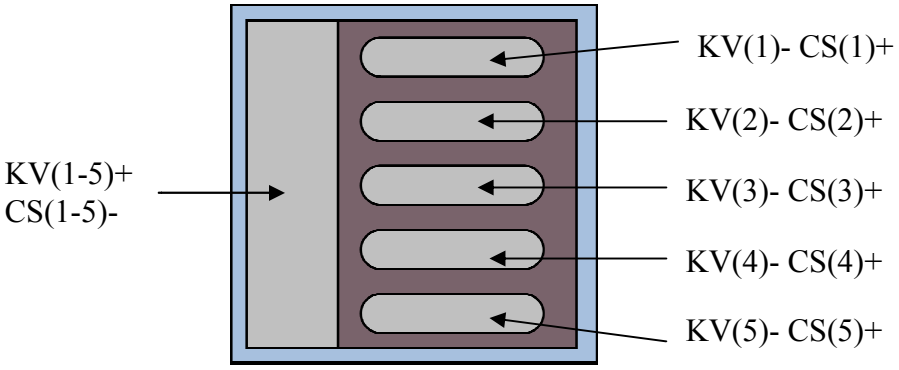

Figure 24: Keithley Voltage (KV) and Current Source (CS) pin numbers and their polarities and their associated connections on the substrate.

The setup system has also been designed in such a way that the lifetime system could be used to measure organic LEDs in addition to photovoltaic devices. To switch between the two setups, space has been left on the substrate holder for a color sensor to measure the intensity of the light produced in addition to the bias voltage across the device. The polarity of the current source must also be switched, as the current must be positive because OLED devices are consuming, rather than producing, power. The current setup of the test system allows for organic photovoltaic and LED devices to be tested at the same time as both devices utilize the same polarity for the Keithley during measurement.

The total number of devices that can be measured at one time is limited by the total outputs the Keithley can measure. This is dependent on both the model and the multiplexer boards within: the Keithley 2700 has 2 slots for multiplexer boards, each of which has a maximum of 40 inputs, and so the limit for the 2700 is 80 inputs. The setup used for prototyping utilized a single multiplexer board with a 20-channel capability; thus the maximum number of devices the prototype system could measure at a single time was 20. For the actual system a Keithley 2750, with slots for up to 5 multiplexer boards, and 3 40-channel multiplexer boards were purchased. Combined with the multiplexer board in the prototype setup, the final setup will have 140-channels, which can measure the lifetime of up to 28 devices simultaneously [66]. The multimeter can read channels at a rate of 200 channels per second, which allows for real time monitoring of voltage degradation regardless of the number of devices being tested.

Characterization of Test System

Upon completion of the prototype test setup, it was important to run characterization experiments to ensure that the system was behaving as intended. The key concerns for the system were to ensure the stability of the output current and to ensure the stability of the LED light sources being used. In addition, experiments were carried out with an amorphous silicon solar cell in ambient air to demonstrate the system was functioning as intended and finally the system was loaded into the glove box and tested with a pentacene/C_{60} device under illumination as a final test of functionality.

Current Stability Experiment

One of the most important aspects of the lifetime test system is the output current as it is this current that is driving the actual device and ensuring its operation at the maximum power point. Any fluctuations in the output current can cause an undesired

change in the bias voltage; thus it is imperative that this current be as stable as possible to ensure that any changes in the voltage are a result of degradation of the device and not a result of instability within the driver board. To ensure stability had been achieved an experiment was designed to test the output current and ensure that there were no variation in the current over a set period of time.

The experiment would attempt to mimic real world use and consisted of all the outputs of a single board connected in parallel. This total current was then connected in series with a resistor. The resistor would mimic the series resistance of the photovoltaic device, which was measured at ~440Ω per device. In order to make it a worst case scenario, the resistance was increased by roughly an order of magnitude to 3.2kΩ per device. Therefore, in the case of the Microsemi board with 5 functional outputs, the resistance value used was 16kΩ. In the case of the Maxim board with 16 outputs the voltage across the resistor would be too high if this worst case scenario was maintained and therefore the resistance was setup to enable the largest possible voltage, which could not exceed VDD of 10V, forcing the resistance value to be 5.56kΩ. This resistance gave a voltage over the resistor of ~9.1V. This setup can be seen in Figure 25.

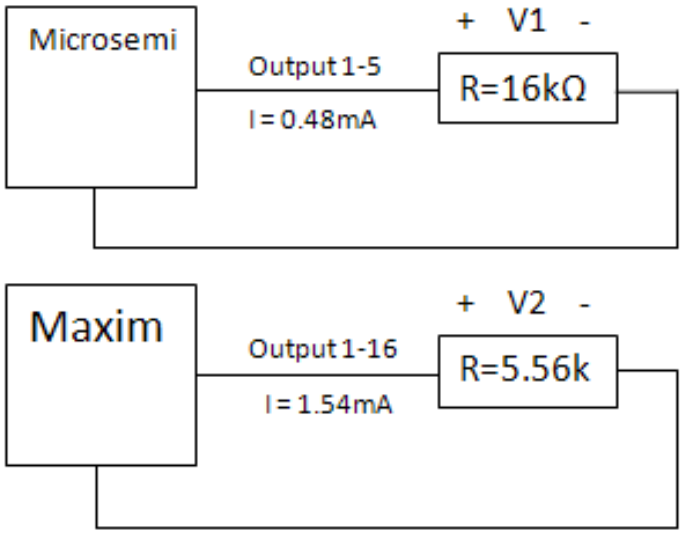

Figure 25: Experimental setup to measure variations in output current.

Both resistors were rheostats that had been set to the correct resistance and measured using a digital multimeter. The experimental setup measured the voltage across each resistor and assumed that any change in current from the board would correspond to a change in voltage across the resistor. It was assumed that the manufacturers tolerance on the resistor, a change of <1%, was negligible; thus if the current output was stable than the voltage across the resistor would not change. The currents were set so that the parallel output of the Microsemi board was 0.48mA or a value of 0.09mA across each of the 5 output sources. This individual output was multiplied by 16 for the Maxim board, for a total output current of 1.54mA over 16 outputs. The plot of Figure 26 shows the results of this experiment after 165 hours of total runtime.

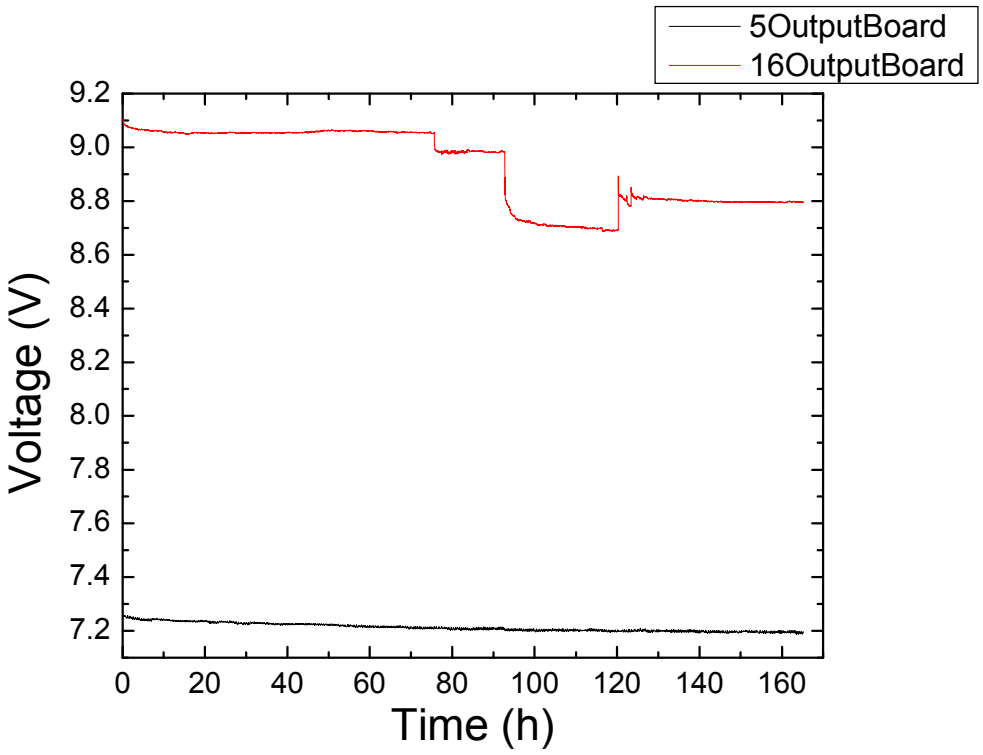

Figure 26: Output voltage over time for Microsemi (5OutputBoard) and Maxim (16OutputBoard) evaluation boards.

From the plot it can be seen that the output current is stable in the Microsemi board with 5 outputs, with a total variation of <1% of the output voltage, implying individual source variation of <0.2%. The Maxim board with 16 outputs is also stable, with a variation of 1.3% until the 97th hour, implying individual source variation of <0.1%. At that point in time the resistor was bumped when checking the experiment causing a decrease in resistance due to the sensitive nature of the rheostat. This decrease caused the steep decline in voltage to 8.7V seen in the graph. The sudden increase around the 120 hour mark was also a result of the rheostat being bumped. The sensitive nature of the rheostat made testing difficult, but it is important to note that after the 97th hour the overall change in voltage was never more than 1% and it must also be pointed out that this decline is across 16 sources, which is three times greater than the 5 sources in the Microsemi board. Thus the experiments confirm that the output of both boards is stable to within <1% per individual current source extrapolated over 1000 hours and therefore any variations in current would have a trivial effect on any experiments on degradation of photovoltaic devices.

It was determined that the Microsemi board would be utilized in future experiments because the microcontroller in the board was more easily obtained then that of the Maxim board. Dr. Dengke Cai has been designing a printed circuit board with 7 of these controllers on the board, along with the associated connectors to easily connect the board to the substrate holder and Keithley. One board would be used on each side of the substrate holder, powering 8 substrates per board, and would allow for simple switching between organic photovoltaic and LED testing. Thus one side of the substrate holder could be testing LEDs while the other side could be testing the lifetime of photovoltaic devices simultaneously.

LED Stability Experiment

The surface mount LED was purchased in a chain of 27 devices on a single substrate, powered by a 1A constant DC current source. The devices were connected in series on the substrate with leads on the end of the substrate to connect another LED chain in series should this be desired. The goal was to create an experiment that would allow us to track any degradation in the LED to determine its stability over time. Because the LED current was constant at 250mA, we assumed any degradation in the LED would manifest itself as an increase in bias voltage across the device. Thus the protective sheathing over a single LED was removed to expose its connections and separate wires were soldered onto its input and output bias voltage points. The LED was then turned on and allowed to run for a period of time while the voltage across the package was recorded. The current was also checked every day and at the end of the experiment in order to ensure that no degradation in the current was also taking place. This was done by connecting a 100Ω resistor onto the positive lead on the end of the LED substrate with the Keithley's probes completing the circuit as shown in Figure 27. It was assumed that because the LEDs are in series, the current recorded would be the same passing through each device. No variations in the current were recorded for the duration of the experiment.

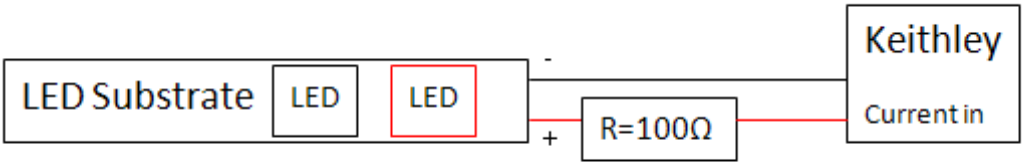

Figure 27: The current is monitored from the end of the substrate connector, with the LED being whose voltage is being monitored is shown in red

The results of the voltage stability experiment are shown in Figure 28. As can be seen from the graph, the LED voltage is stable over a measurement time of 170 hours, with

<0.5% variation over this period. Thus it can be concluded that the LED has degraded very little over this time period and will have a negligible effect on the degradation of photovoltaic cells through loss of irradiance.

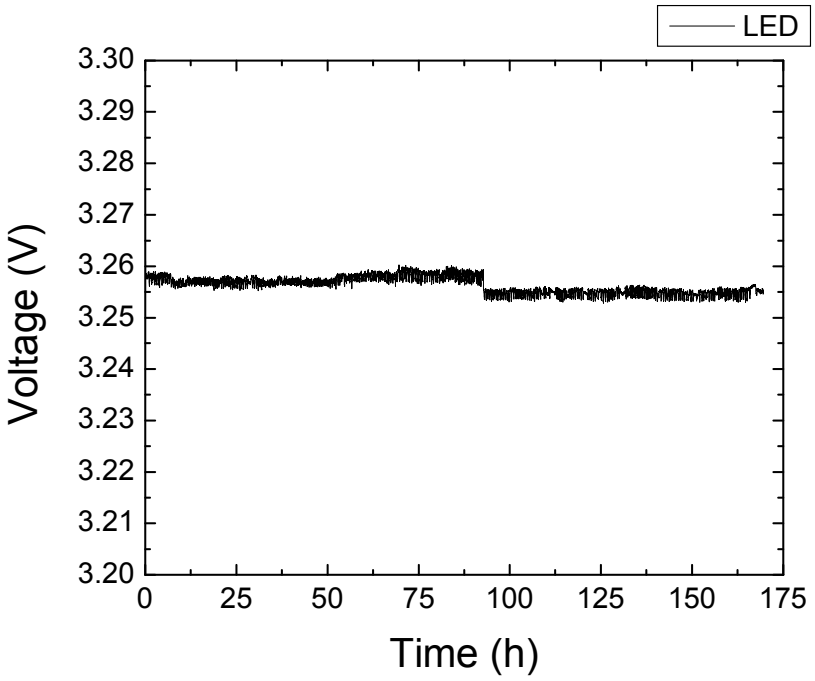

Figure 28: Change in bias voltage of surface mount LED with time at constant current.

Amorphous Silicon Testing

After determining the stability of the LED and output current source a final test was done outside the glove box to ensure the setup worked out as intended. An amorphous silicon solar cell was hooked up to test system and illuminated by the LEDs. The output voltage was plotted over time and allowed to run for several days, to ensure that the system was recording the desired values and operating as intended. The plot in Figure 29 shows the gradual decline in the device with time.

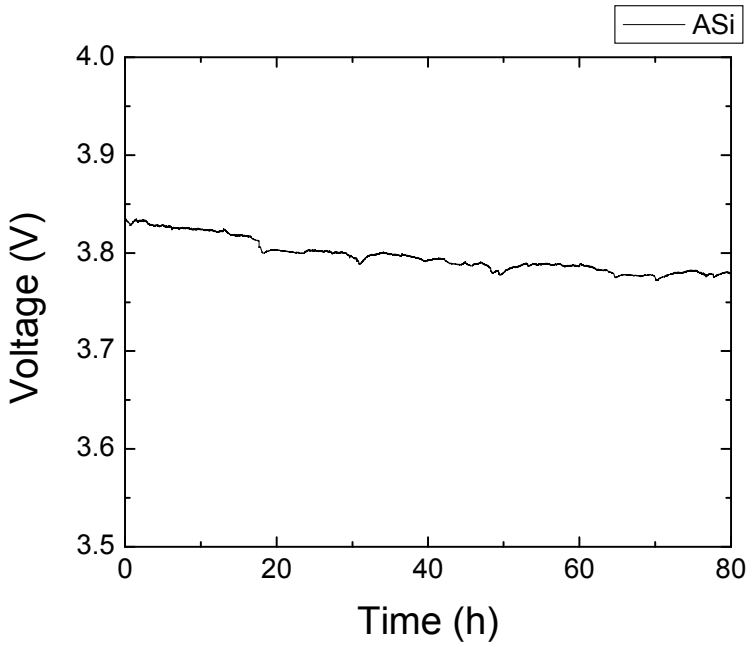

Figure 29: Change in voltage due to degradation over time in an amorphous Si solar cell.

After successful completion of this experiment the system was assumed to be working and thus the only thing that remained was to test it in the glove box on actual pentacene/C_{60} devices.

Pentacene/C_{60} Solar Cell Testing

The goal of this final experiment was to prove that the lifetime setup works in a glove box using organic photovoltaic devices. The system was transferred into a glove box and a pentacene/C_{60} device that had been fabricated for this purpose was loaded into the sample holder. The device had not undergone any surface modifications at all. In order to accelerate the lifetime testing, the surface mount LEDs were not used as the light source; rather a high intensity LED with the same spectrum and irradiance, but with a limited lifetime, was used instead. This was done in order to simulate degradation as none of the main degradation factors were present: the device was in a glove box, preventing

photo-oxidation from occurring, the current densities were only at one sun, preventing charge saturation, and the device was not exposed to any UV light. Thus the change in voltage being recorded, shown in Figure 30, was a result of the LED device decaying down to zero illumination (burn out) by the end of the experiment.

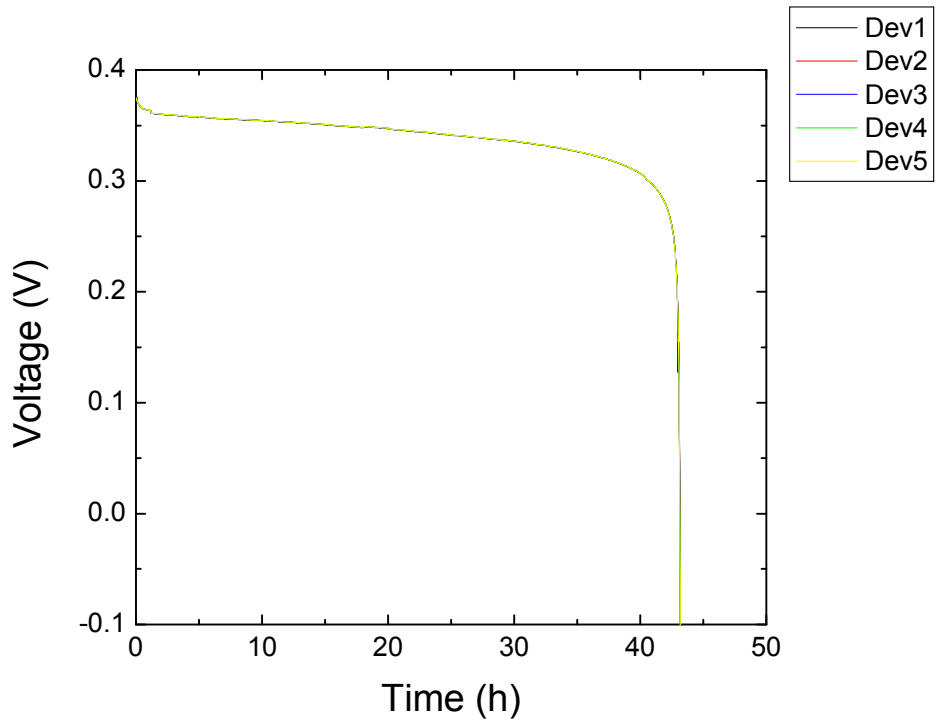

Figure 30: Simulated degradation in 5 pentacene devices on the same substrate using short-lifetime LED light source.

The change in voltage was measured across all five devices on the substrate of the photovoltaic cell. The graph shows identical rates of decay for all five devices creating overlap of all 5 curves, making it difficult to tell them apart. This is consistent with a simulated decay by decreasing the intensity of the LED light source as each device is decaying at the same rate. The decay of the LED remains linear up to the point of failure, where it rapidly decays to zero illumination, causing the sudden drop in voltage. This drop in voltage is consistent with a lack of photocurrent in the device causing it to behave as a diode in reverse bias in order to maintain the negative current, hence the negative

voltage. It can be assumed, therefore, that the test system is fully functional and ready for large scale testing.

Future Setup

Nearly all the equipment required for the assembly and use of the test system has been purchased and is awaiting arrival. The final substrate holders are being machined and the Keithley and multiplexer boards used for the actual measurements have already arrived and are ready for use. The final requirements will be the completion of the printed circuit board by Dr. Cai and its production by Microsemi or another manufacturer. After that the connections between the multiplexer, board and substrate holder will need to be made and the test system will be ready to measure either organic photovoltaic or LED devices.

CHAPTER 4

CONCLUSION AND DISCUSSION

Surface Modified Pentacene Diodes

While it is clear from the data gathered from the pentacene diodes that surface modifications had an effect on the lifetime of the devices, the mechanism for increasing this lifetime remains unclear. The experiments focused on degradation issues related to charge saturation, but further experiments will have to be carried out to determine if this is the same thermal degradation mechanism that occurs when UV light is absorbed by glass substrates. In future experiments testing for this thermal degradation by the use of a thermocouple to monitor the junction temperature would also be suggested and was a key aspect missing from the experiment that was conducted.

While the data seems to indicate a trend with increasing work function for phosphonic acids, this trend does not apply to mechanical surface modification performed with oxygen plasma. The modifications made by the phosphonic acids are not limited to the ITO work function; they also have an effect on the contact angle of the ITO, the angle at which the pentacene vapor meets the ITO interface. It is possible that this change in contact angle can lead to a change in morphology that does not occur with mechanical means such as oxygen plasma. This could be tested in future experiments by selecting phosphonic acids with a large range of contact angles and trying to discern a trend in lifetime.

The key issue with the experimental setup, however, was a statistical issue: the lack of a large sample size for testing. The long durations required for proper lifetime testing severely limited the number of samples being tested, making it very difficult to

notice trends between sample sets because of large standard deviations. The lack of a large-scale test setup required devices to be measured one at a time, greatly delaying the data collection process. This required work on lifetime degradation to be put on hold, until an improved lifetime measurement setup could be created, a project that ended up taking 5 months to complete. Thus any future work on degradation methods will be continued by another student, using the new measurement setup. The next section details some potential experiments that could be conducted with this large scale test setup.

Future Work

The first key experiment that should be conducted is one to determine if high current densities have similar annealing effects as those shown through UV absorption in glass substrates. This experiment would compare the effects of different surface modifications on lifetimes using both degradation methods to see if a similar trend emerges. In addition, the junction temperature could be measured in both cases with a thermocouple to see if similar, localized increases in temperature are taking place. The experiment could also attempt to compare these temperatures and see if the temperature increase caused by the UV can be matched through current saturation and the density of current required to achieve this temperature match. These experiments could be conducted either on pentacene diodes or full devices, although the former would be preferred to allow easier imaging of the ITO-pentacene junction. These images could confirm, or disprove, the idea that both processes cause thermal degradation. If similar pulling back of the pentacene layer was observed in both cases, the cause would likely be thermal annealing.

The exact mechanisms for any improvements via surface modification would also be important to study. As previously mentioned, it would be interesting to re-measure the energy barrier height. Normally it is fixed regardless of surface modification because of Fermi level pinning effects. These effects might be removed, however, when the pentacene pulls away from the ITO interface and a measurement could easily confirm or reject this idea. The changes in series resistance would also be very important in this situation as any pulling away of the pentacene from the ITO interface would result in an increase in contact resistance. By measuring the series resistance, or if possible the contact resistance, it is possible that a model for the change in resistance over time might be created. This model would allow predictions of device lifetime due to this degradation method and would show clear deviations from the model resulting from improvements to the interface.

A final experiment could test the effects of the IR spectrum specifically. While a study found no thermal degradation in the ITO-pentacene interface as a result of IR radiation, the measurements were conducted over only 2 hours. Thus it is possible that for longer time durations with no heat sink or cooling systems that IR radiation could sufficiently heat the electrode to cause thermal degradation. Another experiment could test photovoltaic packaging: if the absorption in the IR spectrum of ITO coated glass is sufficiently small to avoid this effect, it is possible that residual heat from the package could trigger it. Thus an experiment with a common photovoltaic packaging material place on the device coupled with IR radiation could test to see if this effect can be caused by residual heat. A final experiment could attempt to simulate a dessert environment with high temperatures to see if the effect could be caused by indirect thermal interactions.

All these future experiments will benefit greatly from the development of the photovoltaic measurement system because it will allow for the collection of statistically significant data.

Photovoltaic Lifetime Measurement System

The test system that was setup with the assistance of Dr. Dengke Cai will allow for the long term testing of both photovoltaic and OLED devices under a variety of different operating conditions. The most important aspect of the setup is the ability for extremely long operating time periods for a large number of samples for photovoltaic testing through the use of stable, long-lifetime LEDs. The ability to customize the spectrum of the light source by varying the LEDs being used is also an important feature because it allows the user to test key degradation methods in organic materials separately, thus allowing them to isolate the effects of changes in device structure or materials. It also allows the lifetime of 140 devices to be simultaneously tested, allowing statistically significant data to be collected at a faster rate, thus speeding research into new semiconductor and encapsulation materials. In addition, the scalability of the system allows the user to easily increase the number of devices the system is capable of testing through the production of additional substrate holders and driver boards (the schematics of which already exist) and the purchase of additional multiplexer boards and Keithley digital multi-meters. Each additional substrate holder can measure 80 devices and requires only an additional 2 driver boards and 2 multiplexer boards and the associated open slots on a Keithley. Thus the only limit to the number of devices being tested at one time is a monetary and space limitation, rather than a system limitation. The

interoperability of the system between organic LED and photovoltaic devices ensures that test time will never go to waste.

The ability to capture this data in real time allows researchers more data points in order to fully understand the rate of degradation and give insight into how these rates can be modeled in the future. The modular aspect of the system also allows testing to take place in nearly any environment with access to a computer and power source, whether it is in a glove box, in ambient air, or even outside. Finally, the ability to operate the photovoltaic devices in a manner that is similar to their real world applications allows the user to gain insight into problems that may only exist in these settings.

Future Work

The current test setup is a prototype of the final system and therefore certain things must be accomplished in order for the final system to be ready for use. While the new multiplexer and source measurer have been purchased, they will need to be assembled and the connections will need to be made between the substrate holders that are currently being machined and the multiplexer boards. These connections will be made via a specifically designed driver board, but this board is still currently being designed and is not yet ready for production. In addition, the creation of a separate driver board for the LED light sources would be recommended. The current system using an LED lighting strip does not allow for efficient placement of the LEDs to ensure optimum light absorption by the photovoltaic device because the spacing between LEDs is fixed. This spacing was determined by the manufacturer and not optimized to our current test setup. A separate driver board for the LED would allow the user to determine LED spacing for optimum light coverage and should include UV LEDs in addition to white LEDs. These

two sets should be able to be independently selected, allowing the user to choose between one or the other, or both, depending on the requirements of the experiment. Upon completion of these two final driver boards the final test setup can be assembled. This setup will need to be characterized as well, although this can be done by following the procedures outlined in the characterization of the test system. Similar results should be obtained, whereupon the system will be fully functional and ready for experimentation.

REFERENCES

[1] B. KIPPELEN, ECE6540A, Organic optoelectronics. Lecture notes, Georgia Institute of Technology, School of Electrical and Computer Engineering, 2010.

[2] C. K. CHIANG, C. R. FINCHER JR., Y. W. PARK, A. J. HEEGER, H. SHIRAKAWA, E. J. LOUIS, S. C. GAU, A. G. MACDIARMID, "Electrical Conductivity in Doped Polyacetylene," *Phys. Let. Rev.* **39**, no. 17, pp. 1098–1101, 1977.

[3] S.A. Jenekke and K. J. Wynne, *Photonic and Optoelectronic Polymer.* ACS Symposium Series 672, 1997.

[4] T. A. Skotheim and J. R. Reynolds, *Conjugated Polymers: Theory, Synthesis, Properties, and Characterization.* 3rd ed. London: CRC Press, 2007.

[5] R. F. Pierret, *Semiconductor Device Fundamentals.* 2nd ed. London: Addison Wesley, 1996.

[6] Renewable Resource Data Center, "AM1.5 Global Spectrum," *US National Renewable Energy Laboratory*, [Online] Available: rredc.nrel.gov/solar/spectra/am1.5 [Accessed: March 2010].

[7] P. Sullivan and T.S. Jones, "Pentacene/fullerene (C_{60}) heterojunction solar cells: Device performance and degradation mechanisms," *Org. Elec.* **9**, 656-660, 2008.

[8] J. E. Mark, *Physical Properties of Polymers Handbook.* 2nd ed. New York: Springer, 2007.

[9] M. A. Fox and J. K. Whitesell, *Organic Chemistry.* 2nd ed. Boston: Jones and Bartlett, 1997.

[10] B. Kippelen and J. Brédas, "Organic Photovoltaics," *Energy Enviorn. Sci.* **2**, 251-261, 2009.

[11] C.D. Dimitrakopoulos and P.R.L. Malenfant, "Organic thin film transistors for large area electronics," *Adv. Matter* **14,** 2002.

[12] "List of Cell Phones with Organic LED Displays," *Organic LED Information Database,* [Online] Available: www.oled-info.com/devices [Accessed: May 2010].

[13] PC World, "OLED: New Star of the Small Screen," *PC World Magazine Online,* [Online] Available: www.pcworld.com/article/119722/oled_new_star_of_the_small_screen.html [Accessed: May 2010].

[14] M. A. Green, K. Emery, Y. Hishikawa, and W. Warta, "Solar Cell Efficiency Tables," *Prog. Photovolt: Res. Appl*. **18,** 144–150, 2010.

[15] Energy Information Administration, "World Total Primary Energy Consumption," *US Department of Energy,* [Online] Available: eia.doe.gov/oiaf/ieo/pdf/ieoreftab_1.pdf [Accessed: March 2010].

[16] "DOE Solar Energy Technologies Programs," *US Department of Energy*, DOE/GO-102006-2314, May 2006.

[17] Energy Information Administration, "Photovoltaic Shipments," *US Department of Energy,* [Online] Available: eia.doe.gov/cneaf/solar.renewables/page/solarreport/table3_6.pdf [Accessed: March 2010].

[18] S. Yoo, W. Potscavage Jr., B. Domercq, S.C. Jones, R. Szoszkiewicz, D. Levi, E. Riedo, S. Marder, and B. Kippelen, "Analysis of improved photovoltaic properties of pentacene/C_{60} organic solar cells: Effects of exciton blocking layer thickness and thermal annealing," *Solid-State Elec.* **51,** 1367-1375, 2007.

[19] J. Xue, B.P. Rand, S. Uchida, and S.R. Forrest, "Mixed donor-acceptor molecular heterojunctions for photovoltaic applications," *J. Appl. Phys.* **98**, 2005.

[20] J. Puigdollers, C. Voz, A. Orpella, I. Martin, M. Vetter, and R. Alcubilla, "Pentacene thin-films obtained by thermal evaporation in high vacuum," *Thin Solid Films* **427**, 367-370, 2003.

[21] W. Potscavage Jr., A. Sharma, and B. Kippelen, "Critical Interfaces in Organic Solar Cells and Their Influence on the Open-Circuit Voltage," *Accts. Chem. Res.* **42** no. 11, 1758-1767, 2009.

[22] A.K. Pandey, S. Dabos-Seignon, J.M. Nunzi, *Appl. Phys. Lett*. **89** (2006) 113506.

[23] S. Forrest and P. Peumans, "Solar Cells using Fullerenes," U.S. Patent 6580027, June 11, 2001.

[24] M. Koehler, M.C. Santos, and M.G.E. da Luz, "Positional disorder enhancement of exciton dissociation at donor/acceptor interface," *J. Appl. Phys.* **99**, 2006.

[25] A. Kahn, N. Koch, and W. Gao, "Electronic Structure and Electrical Properties of Interfaces Between Metals and π-Conjugated Molecular Films," *J. Poly. Sci.:Part B: Poly. Phys.* **41**, 2529-2548, 2003.

[26] "Basic Research Needs for Solar Energy Utilization," *US Department of Energy*, Available Online: www.sc.doe.gov/bes/reports/files/SEU_rpt.pdf., April 2005.

[27] M.A. Green, *Solar Cells,* Englewood Cliffs: Prentice-Hall, 1998.

[28] P. Sullivan, S. Heutz, S.M. Schultes, T.S. Jones, *Appl. Phys. Lett.* **84** (2004) 1210.

[29] J.G. Xue, B.P. Rand, S. Uchida, S.R. Forrest, *Adv. Mater.* **17** (2005) 66.

[30] S. Heutz, P. Sullivan, B.M. Sanderson, S.M. Schultes, T.S. Jones, *Sol. Energy Mater. Sol. Cells* **83** (2004) 229.

[31] V.Y. Butko, X. Chi, D.V. Lang, and A.P. Ramirez, "Limit of Field Effect Mobility on Pentacene Single Crystal," *Los Alamos National Labs*, 2003.

[32] B. Kippelen, S. Yoo, B. Domercq, and W. Potscavage Jr., "Organic solar-cell efficiency boosted using polycrystalline pentacene films," *SPIE Newsroom* **10.1117/2.1200601.0077** 2006.

[33] A.K. Pandey, J.M. Nunzi, *Appl. Phys. Lett.* **89** (2006) 213506.

[34] F. de Angelis, M. Gaspari, A. Procopio, G. Cuda, and E. Di Fabrizio, "Direct mass spectrometry investigation on Pentacene thin film oxidation upon exposure to air," *Chem. Phys. Let.* **468**, 193-196, 2009.

[35] A. Maliakal, K. Raghavachari, H. Katz, E. Chandross, T. Siegrist, *Chem. Mater.* **16** (2004) 4980.

[36] M. Yamada, I. Ikemoto, H. Kuroda, Bull. *Chem. Soc. Jpn* **61** (1988) 1057.

[37] I.C. Lewis, L.S. Singer, *J. Phys. Chem.* **85** (1981) 354.

[38] A. Vollmer, H. Weiss, S. Rentenberger, I. Salzmann, J.P. Rabe, N. Koch, *Surf. Sci.* **600** (2006) 4004.

[39] F. De Angelis, Gobind Das, E. DiFabrizio, *Chem. Phys. Lett.* **462** (2008) 234.

[40] S.S. Palayangoda, R. Mondal, B.K. Shah, D.C. Neckers, *J. Org. Chem.* **72** (2007) 6584.

[41] S.H. Chan, H.K. Lee, Y.M. Wang, N.F. Fu, X.M. Chen, Z.W. Cai, and H.N.C. Wong, "A soluble pentacene: synthesis, EPR, electrochemical studies of 2,3,9,10-tetrakis (trimethylsilyl)pentacene," *Chem. Commun.* 66-68, 2005.

[42] J. Pflaum, J. Niemax, A.K. Tripathi, *Chem. Phys.* **325** (2006) 152.

[43] W.J. Potscavage Jr., S. Yoo, B. Domercq, B. Kippelen, *Appl. Phys. Lett.* **90** (2007) 253511.

[44] S. Yoo, B. Domercq, B. Kippelen, *Appl. Phys. Lett.* **85** (2004) 5427.

[45] N. Kim, W. Potscavage Jr., B. Domercq, B. Kippelen, S. Graham, *Appl. Phys. Lett.* **94** (2009) 163308.

[46] F.J.M.Z. Heringdorf, M.C. Reuter, R.M. Tromp, *Nature* **412** (2001) 517.

[47] C.C. Mattheus, G.A. de Wijs, R.A. de Groot, T.T.M. Palstra, *J. Am. Chem. Soc.* **125** (2003) 6323.

[48] A. Niemegeers, M. Burgelman, *J. Appl. Phys.* **81** (1997) 2881.

[49] P. Yu, C.H. Chang, M.S. Su, M.H. Hsu, K.H. Wei, *Appl. Phys. Lett.* **96** (2010) 153307.

[50] J. Xue, S. Uchida, B.P. Rand, and S.R. Forrest, "4.2% efficient organic photovoltaic cells with low series resistance," *Appl. Phys. Lett.* **84** no.16, 3013-3015, 2004.

[51] A. Sharma, B. Kippelen, P.J. Hotchkiss, S. Marder, *Appl. Phys. Lett.* **93** (2008) 163308.

[52] A. Sharma, A. Haldi, W. Potscavage Jr., P. Hotchkiss, S. Marder, and B. Kippelen, "Effects of surface modification of indium tin oxide electrodes on the performance of molecular multilayer organic photovoltaic devices," *J. Mater. Chem.* **19**, 5298-5302, 2009.

[53] A. Sharma, A. Haldi, P. Hotchkiss, S. Marder, B. Kippelen, *J. Appl. Phys.* **105** (2009) 074511.

[54] C.C. Wu, C.I. Wu, J.C. Sturm, A. Kahn, *Appl. Phys. Lett.* **70** (1997) 111348.

[55] S. Fujita, T. Sakamoto, K. Ueda, K. Ohta, and S. Fujita, "Surface Treatment of Indium-Tin-Oxide Substrates and Its Effect on Initial Nucleation Processes of Diamine Films," *Jpn. J. Appl. Phys.* **36**, 350-353, 1997.

[56] F. De Angelis, S. Cipolloni, L. Mariucci, G. Fortunato, *Appl. Phys. Lett.* **88** (2006) 193508.

[57] F. Krebs and K. Norrman, "Analysis of the Failure Mechanism for a Stable Organic Photovoltaic During 10000 h of Testing," *Prog. Photovolt: Res. Appl.* **15**, 697-712, 2007.

[58] International Electrotechnical Commission for Electrical Equipment, "List of Photovoltaic Standards". [Online] Available: http://members.iecee.org/iecee/ieceemembers.nsf/IECEEScopeInStandardByCat?ReadForm&PC=PV [Accessed: March 2010].

[59] Energy Information Administration, "Solar Photovoltaic Resource Potential," *US Department of Energy,* [Online] Available: www.eia.doe.gov/cneaf/solar.renewables/ilands/fig11.html [Accessed: March 2010].

[60] E.A. Katz, S. Gevorgyan, M.S. Orynbayev, and F.C. Krebs, "Out-door testing and long-term stability of plastic solar cells," *Eur. J. Appl. Phys.* **36**, 307-311, 2007.

[61] M. Jørgensen, K. Norrman, and F.C. Krebs, "Stability/degradation of polymer solar cells," *Solar Energy Materials and Solar Cells* **92**, 686-714, 2008.

[62] S.A. Gevorgyan, M. Jørgensen, and F.C. Krebs, "A setup for studying stability and degradation of polymer solar cells," *Solar Energy Materials and Solar Cells* **92**, 736-745, 2008.

[63] National Climactic Data Center Online, "Local Weather Cloud Coverage," *US National Oceanic and Atmospheric Association*. [Online] Available: lwf.ncdc.noaa.gov/oa/climate/online/ccd/cldy.html [Accessed: March 2010].

[64] "Manufacturers Data Sheet," Cree Incorporated, 2007.

[65] S. Yoo, "Organic Solar Cells Based on Liquid Crystalline and Polycrystalline Thin Films," Ph.D. dissertation, University of Arizona, Tucson, AZ, USA, 2005.

[66] "Keithley 2750 Data Sheet," *Keithley Instruments Inc*, [Online] Available: www.keithley.com/data?asset=9498 [Accessed: February 2010].